ASEAN Project on Disaster Risk Reduction by Integrating Climate Change Projection into Flood and Landslide Risk Assessment

Technical Report on Integrating Climate Change Projection into Landslide Risk Assessment

Case Study: Taunggyi River Basin Pilot, Shan State of Myanmar

Japan-ASEAN Integration Fund (JAIF)
ASEAN Committee on Disaster Management (ACDM)

Implemented by

ABSTRACT

This case study was conducted as part of the ASEAN Project on Disaster Risk Reduction by Integrating Climate Change Projection into Landslide Risk Assessment (ASEAN DRR-CCA). Its main purpose is to showcase application of the methodologies described in the guidelines developed as part of this project. The study area is the Taunggyi River Basin, located in Shan State Province of Myanmar. A similar study under the same project was also done in the Phoukhoun River Basin, Lao PDR.

The hazard, exposure, vulnerability and capacity assessment approach adopted in this case study is based on definitions from UNDRR (formerly known as UNISDR). It should be noted that the landslide hazard definition used in this case study refers to *landslide susceptibility*, which is defined as spatial likelihood or probability for a landslide to occur in the future, and no information on magnitude (size/volume and velocity) was available or provided due to lack of data needed to carry out the hazard assessment covering the study area.

A bivariate statistics analysis using weight of evidence was used for landslide susceptibility mapping. The methodology relies on an inventory of landslide locations that were obtained from satellite images covering the study area, combined with controlling factors such as slope, distance to road and river network, land use, land cover and geological features. The majority of the data used for this study was collected from the public domain (freely available data). Based on the weight of evidence, GIS datasets were combined using weighted overlay techniques to create the landslide susceptibility map. This study used 2 IPCC scenarios of representative concentration pathways (RCPs) in three different time periods: the 2030s, 2050s, and 2080s. Results indicate a trend of landslide increases in susceptible areas for each time period for both IPCC scenarios of RCP 4.5 and RCP 8.5.

A landslide vulnerability assessment is a complex process that should consider multiple dimensions and aspects, including both physical and socioeconomic factors. A vulnerability assessment for this case study was completed through a sampling of surveyed households located in high and very high susceptible zones.

Landslide susceptibility map spatial distribution was integrated with vulnerability to obtain the spatial distribution of risk. Analyses indicated that highly susceptible and highly vulnerable households do not demonstrate a high level of risk individually, though a combination of them does. Landslide risk was assigned five classes: very high, high, moderate, low and very low. Two-hundred households were surveyed. Of the 171 samples that were located inside the river basin, there were 60 and 35 households were identified as very high risk and high risk respectively. Three classes – moderate risk, high risk, and very high risk -- made up 76.6 percent of the household sample total. If the sampling number is increased, households at risk are also likely to increase.

This risk assessment provides essential information, and outputs are useful for a better understanding of potential impacts caused by landslide. A better disaster risk reduction strategy can therefore be initiated/developed or enhanced, and efforts for the reduction and mitigation of future landslide hazards can be prioritized. This study also concluded that the developed approach and methodologies are applicable and can be updated when new data becomes available in the future.

TABLE OF CONTENTS

LIST OF FIGURES

List of Tables

1. Introduction to Landslide Hazard Risk Assessment Methodology

1.1 Introduction

It is generally understood that disaster risk management should be based on an understanding of disaster risk in all its dimensions, including vulnerability, capacity, exposure of persons and assets, and hazard characteristics. **Figure 1.1** Below shows the basic concept of landslide hazard and risk assessment and its application in disaster risk reduction and management.

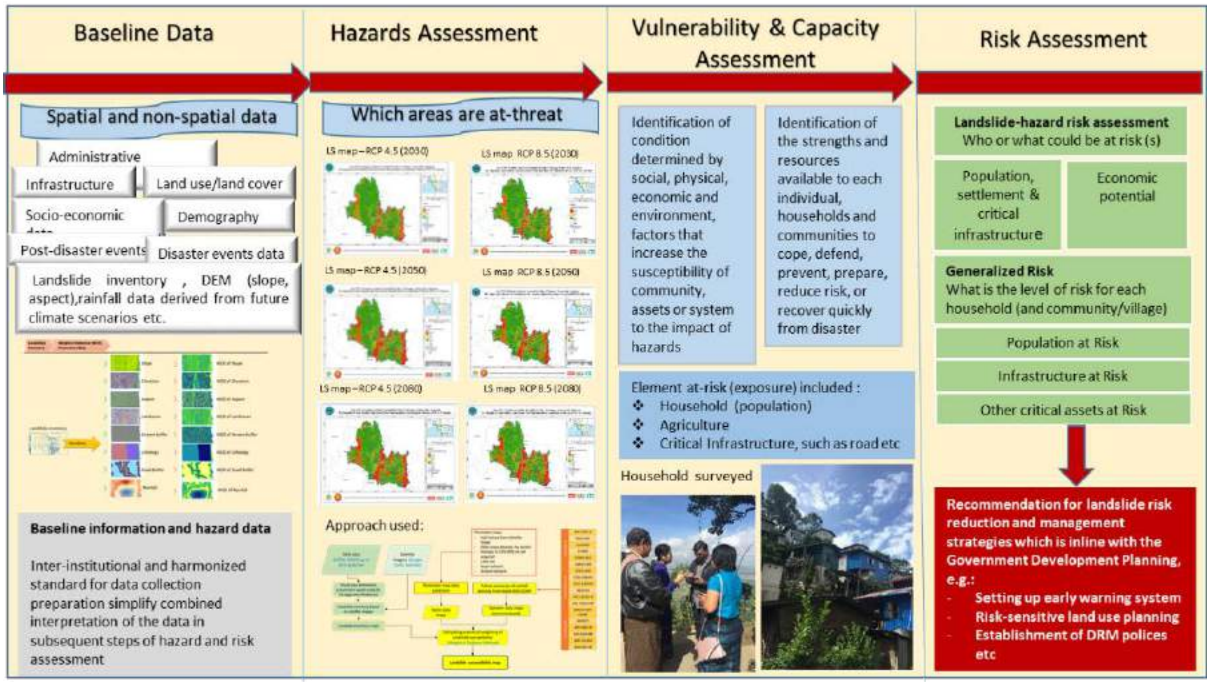

Figure 1.1 Flowchart showing the role of risk assessment in disaster risk management

A risk assessment has to be completed based on the understanding defined by UNISDR that disaster *risk* is the potential loss of life, injury, or destroyed or damaged assets which could occur to a system, society, or a community in specific period of time determined probability as a function of hazard, exposure, vulnerability and capacity.

From a disaster risk reduction lens, the risk is defined as:

$$Risk = Hazard \times Vulnerability/Capacity.$$

Based on the above concept, the disaster risk assessment for this case study has been prepared based on the following basic equation:

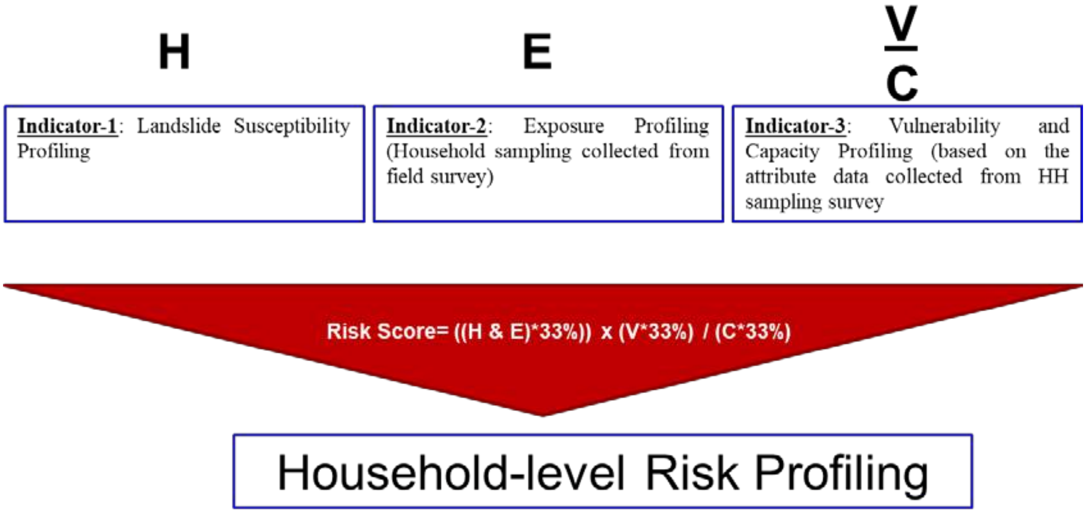

Figure 1.2 Basic formula used for calculating the household risk profile in this case study

Each indicator described in the above basic equation is discussed in the following subsections.

1.2 Study Area Background

In the past, Myanmar had been considered a country relatively safe from natural disasters. However, that understanding gradually started changing with the devastation created due to cyclone Nargis in early May 2008, the worst natural disaster in the country's recorded history. In the recent past, several significant disaster events have been reported in various parts of Myanmar and floods, cyclones, drought and landslides have become common disaster events that have had serious impacts on day-to-day life of the people and the country's national economy.

The context in Shan State, where the Taunggyi RBP study area is located, is similar. Except in the area covered by the capital city Taunggyi and other urban areas in the vicinity, the state is largely rural. Myanmar's buildings, lifestyle, cultural practices and natural environment may have well synchronized to create an environment relatively less vulnerable to natural disasters in the past. However, that general understanding appears to be changing fast with the current urbanization trends and associated development activities. This may have been further aggravated due to climate change and climate variability observed on the Asia subcontinent. Among the common hazards observed within the area, floods are considered the most important in terms of damage, followed by landslides. Landslides are increasingly becoming one of the major threats and present dangers to humans, infrastructure, lifeline facilities and assets. The present level of landslide risk may not be very high, but it can grow and become higher in the future if landslide potential is ignored and proper precautionary measures to mitigate that potential are not taken by the authorities. The prevailing landslide hazard risk observed in this area is due to several factors, natural as well as human-made, and is triggered predominantly due to higher precipitation events.

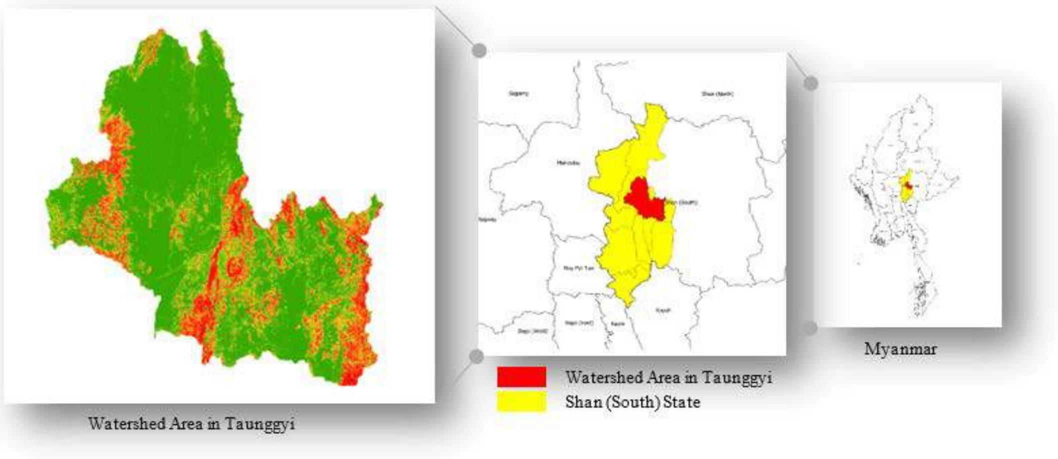

Figure 1.3 Study Area, Taunggyi RBP in the Shan State of Myanmar

Among the natural factors that play a major role in landslide initiation is the geological as well as geotechnical characteristics of the bedrock and overburdened soil formations. Shan State has relatively high mountains in the north, with the south mostly confined to a hilly plateau. Topographically, the hill ranges are rugged and constitute several peaks, gorges and valleys. Rock types seen in the vicinity of the capital city and surrounding area consist of formations of a succession of thick-bedded limestone, siltstone and dolomites. The different types of rock formations behave differently depending on the changes they have historically undergone over the years. Some of the extensively developed upland hill ranges that consist of Plateau limestone exhibit higher resistance to weathering and show more stability. They form dissected escarpments and slopes with a higher gradient and are represented as isolated peaks as well as mountain ranges. On the other hand, the highly brecciated dolomitic limestone formations that are often inter-bedded with siltstone and limestone create weak structures on exposed slopes, particularly when they are present on medium to steep slopes that are often associated with roads and highways. These areas often tend to destabilize during higher precipitation events.

This phenomenon can be seen quite often on the Taunggyi–Loilem highway. The cutting failures and major landslides observed along this road are due to the presence of highly brecciated formations. In addition, failures observed along the road can also be attributed to a thick overburdened cover comprised of colluvium and residual soil formations, as well as highly fractured rock masses. Landslides associated with this road network can cause frequent traffic hold-ups on the affected roads, and this creates direct economic impact due to transportation disruptions. Moreover, it frequently creates inconvenience to road users and the wider community. The cost of road rehabilitation and landslide mitigation work is also high, and can account for a considerable percentage of road sector annual emergency maintenance costs.

Very dense settlements have become a common feature in the capital city of Taunggyi and other urban areas in the vicinity. Some of them are located on hill tops and neighboring sloping ground that consists of a shallow soil overburden. In most cases, underlying bedrock formations are dolomite or limestone and the overburden thickness is limited to a few meters only. Already several minor landslides and destabilizations affecting a several houses have been reported in these urban settlements. In a few cases loss of life has been reported, for example, near the Kyaung Gyi Su Quarter, Area 8, Gandama Street, Area 7, near Aung Mingalar Temple, Nyaung Phyu Sa Khan Quarter, etc. The majority of the building stock in these settlements consists of either solid reinforced concrete (RC) structures or block masonry buildings that appear structurally solid. Lightweight structures constructed using bamboo panels appear to be weaker and more vulnerable, though there are fewer of these.

The general perception of the communities in Taunggyi Township and other urban areas in the area is that impacts of the majority of the hydro-meteorological disaster events such as floods, landslides, etc. have increased in recent years, possibly due to climate change.

The above highlighted facts reveal the possibility of an increase of potential risk and vulnerability to landslides in the future that will affect several sectors such as urban settlements, highways and infrastructure, agriculture, the economy, etc. This also demonstrates the appropriateness of undertaking a comprehensive landslide risk assessment based in Shan State, as well as the need for an analysis of the influence of climate change with focus on the spatial and temporal dimensions of potential landslide risk. It additionally highlights the need to build capacity within Shan State agencies for undertaking necessary efforts for risk minimization in the near future.

2. Landslide hazard and risk assessment used in this case study

2.1 Landslide Susceptibility Mapping

The main conditional factors (static maps) considered for susceptibility mapping were:

- Lithology
- Land use and land cover
- Slope
- Aspect
- Road network
- Stream network
- Landslide inventory

And the causative factor (dynamic maps) considered was rainfall derived from climate projection scenarios. The methodology adopted in this study is shown in **Figure 2.1**.

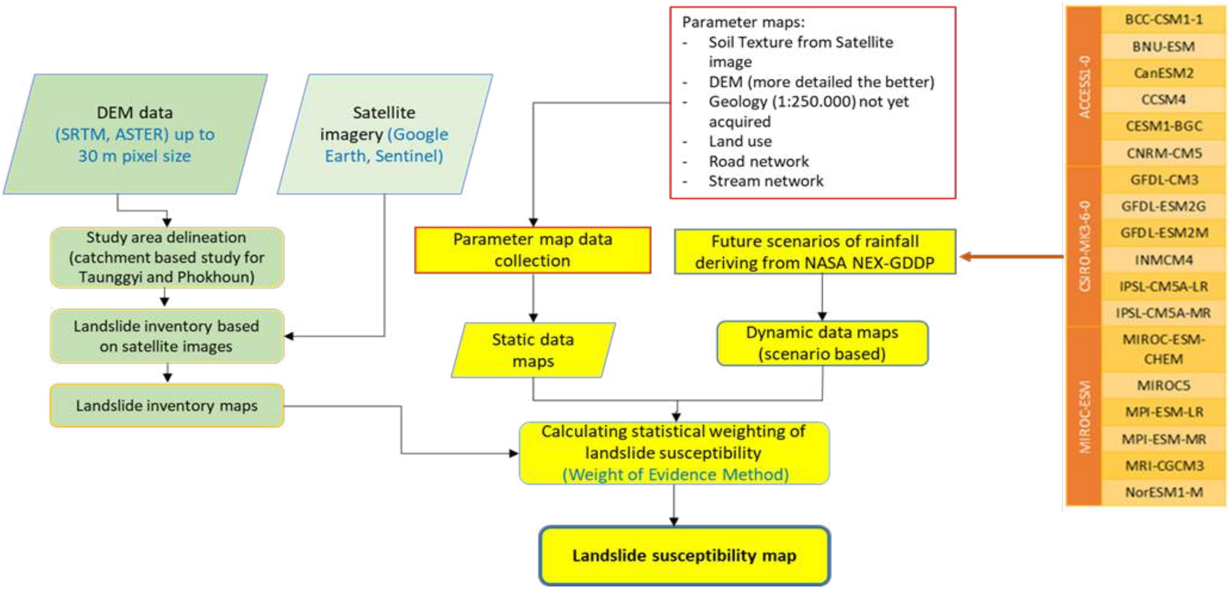

Figure 2.1 Landslide susceptibility analysis flowchart using Weight of Evidence

The detailed discussion of landslide susceptibility mapping can be referred to in the following subsections that start with baseline data preparation, deriving rainfall data from climate scenarios and landslide susceptibility mapping.

2.1.1 Data preparation conditional factors and parameters

Data and information are fundamental for reliable landslide susceptibility mapping as the assessment process is data intensive. Data gathering requires a great deal of effort. Alternative approaches to treat gaps must be found if data and information is unavailable.

Geospatial data mainly covers lithology, topography (elevation, slope and aspect), stream networks, land use and land-cover maps, road networks, etc. Preparation and analyses have been done in a GIS environment, and the results are presented as maps.

The spatial data for conditional factors and parameters was obtained in a GIS environment using QGIS as discussed in the following section below.

(1) Slope gradient

Slope is a measure of steepness using a degree of inclination relative to the horizontal plane. It is typically expressed as a percentage, an angle, or a ratio. Slope gradient can be generated from the Digital Elevation Model (DEM) of a 30-meter pixel Shuttle Radar Topography Mission (SRTM). Before generating a slope gradient, the map projection needs to be translated into a specific geographical area UTM (meter units), for example UTM zone 47N (for Myanmar).

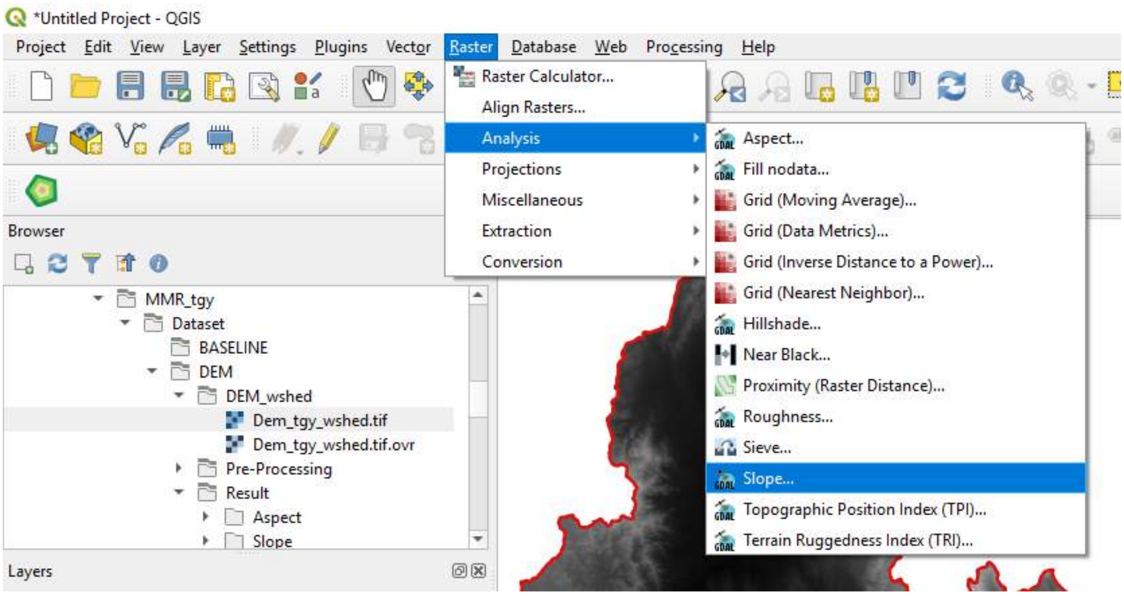

Figure 2.2 Slope gradient processing

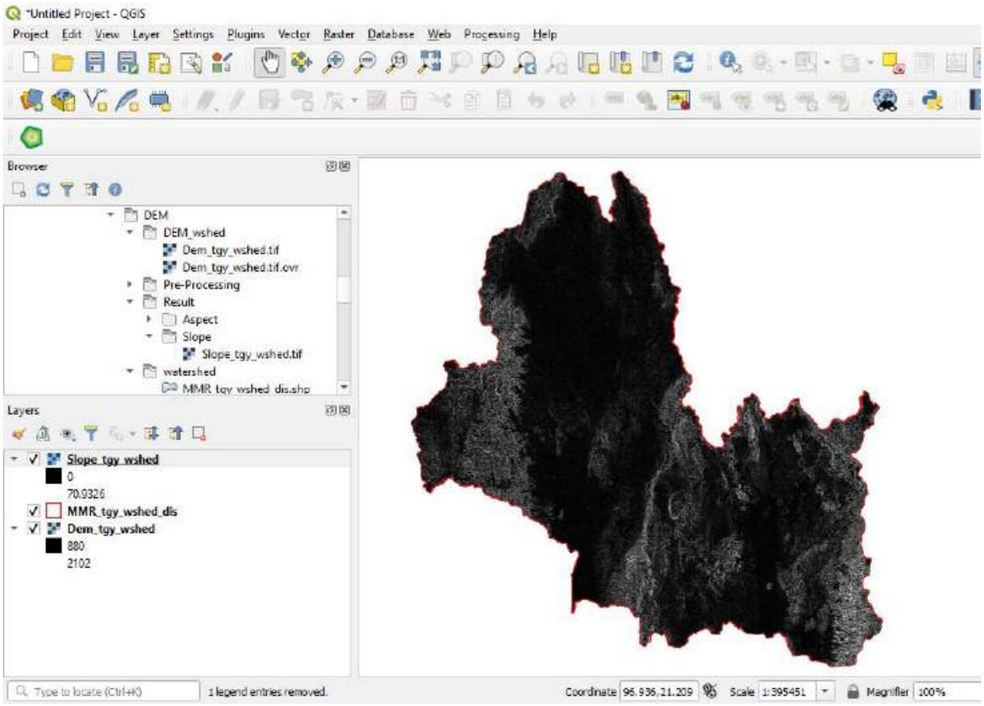

Figure 2.3 Slope gradient classification

The slope gradient varies from 0° to approximately 71.93° within the watershed area as seen in the picture above. The mean slope value is 7.88°, with a standard deviation around 7.95.

Slope Classification

1. Slope gradient is reclassified into 15 classes for the landslide susceptibility analysis.
2. Right click the slope layer from the Table of Contents and select Layer properties.
3. Change the render type to “Singleband pseudocolor”.
4. Change the classification mode to “Equal Interval” and type “15” classes.
5. Select the color ramp.

(2) Slope aspect

Slope aspect is also known as slope orientation or slope azimuth. It represents the direction of a slope. Aspect can be classified according to the slope angle with a descriptive direction. An output aspect raster (horizontal lines composed of individual pixels) will typically result in several slope direction classes. Aspect is measured clockwise starting north at 0° and returning back to 360° north. After running the aspect tool, the output raster symbolizes aspect direction based on slope angle. Each slope direction will represent a slope angle range.

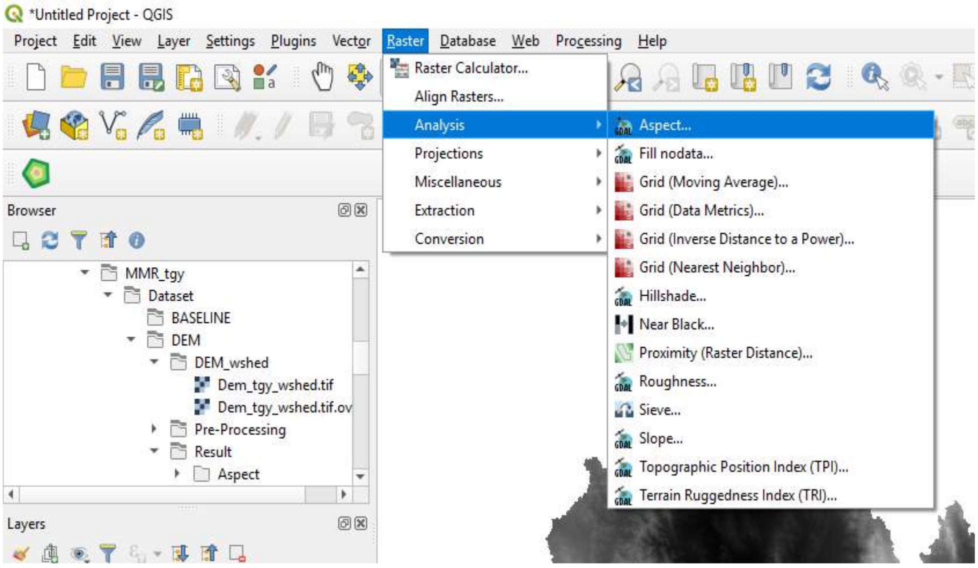

Figure 2.4 Aspect Processing in QGIS

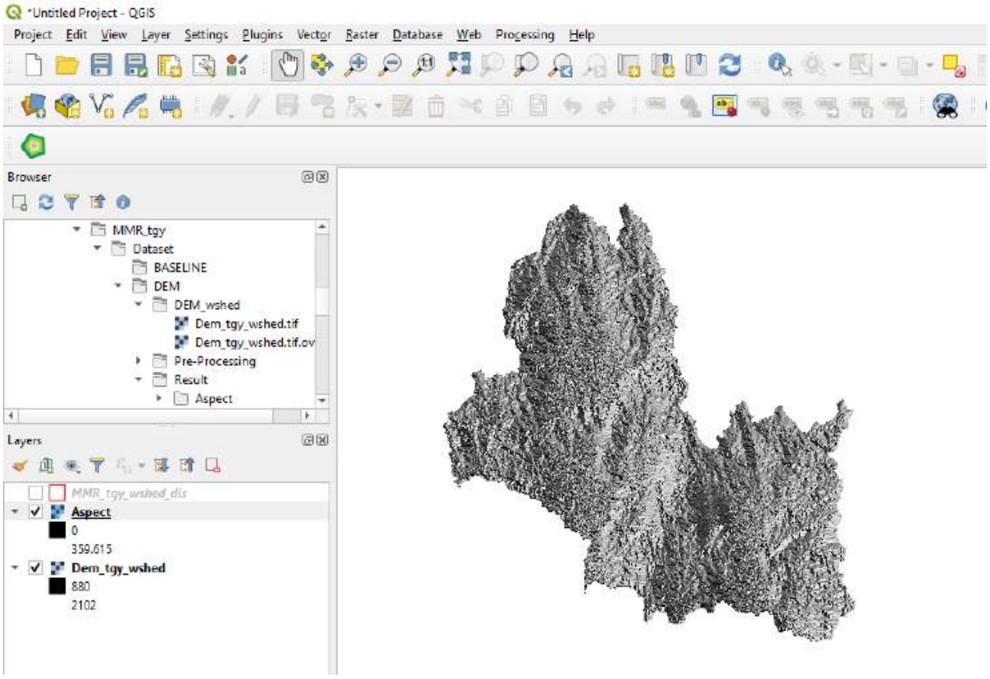

Figure 2.5 Slope Aspect

Aspect is made up of the grey cells in the aspect map where slope exists. It is measured clockwise starting north at 0°and returns back to 360° north. After running the aspect tool, the output raster symbolizes aspect direction based on slope angle. Each slope direction will represent a slope angle range. Reclassifying the aspect map can be done by changing the symbolism and setting the number of classes.

Aspect classification

1. Aspect is reclassified into 9 classes for the landslide analysis.
2. Right click the slope layer from the Table of Contents and select layer properties.

3. Change the render type to “Singleband pseudocolor”.
4. Change the classification mode to “Equal Interval” and type “9” classes.
5. Select the color ramp.

(3) Distance from road

Proximity to roads is also considered a potentially important factor because road construction usually includes land or material excavation in slope areas and the addition of land or materials to the slope in other areas. This might result in slope line changes, artificial slope creation or road cuts that might be affected by landslide activities (Che et al., 2011). Proximity to road was regrouped into four classes (25m,50m,100m, and 150m) using the multiple ring buffer tool in the GIS environment.

(4) Distance from river

Proximity to a river may adversely affect slope stability due to slope toe undercutting, or saturation in the lower part of the slope, resulting in a water level increase.

(5) Land use and land cover

A land use and land cover map can be derived from processing satellite imagery, such as Landsat, or can be obtained from existing maps kept by relevant agencies. In this study, the land use and land cover maps were derived from the regional land cover monitoring system developed by the SERVIR-Mekong program. SERVIR-Mekong has produced a series of annual land cover maps with multi-purpose typologies using Landsat images from 2000-2017 at a 30-meter resolution.

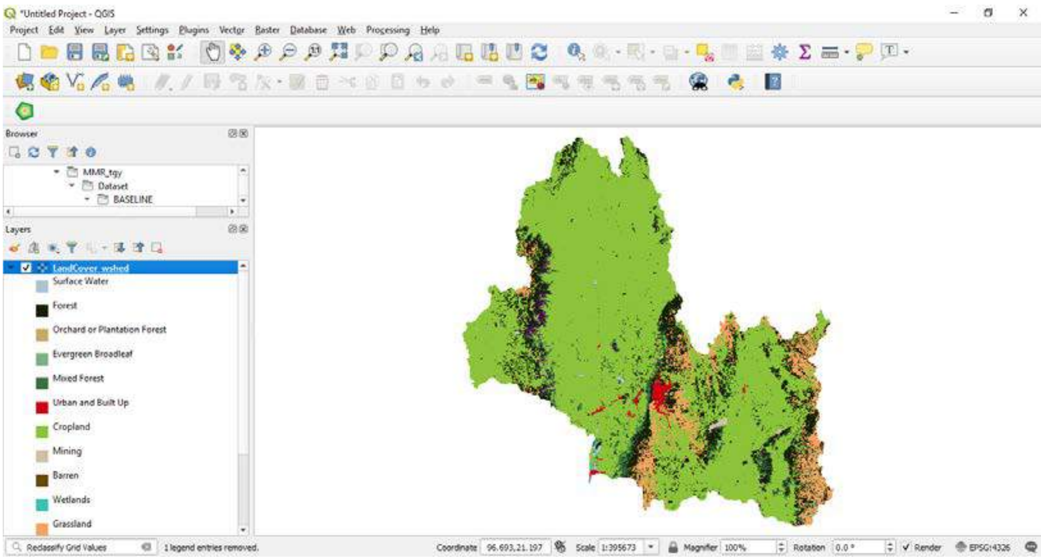

Figure 2.6 Taunggyi land use

(6) Hydro-meteorological datasets

Hydro-meteorological data consists of a precipitation (mainly rainfall) time-series. Additionally, temperature and humidity can often be collected from ground observation stations, as well as remote sensing sources. In this study, rainfall datasets that were used for the RBPs were derived from historical climate data and future climate projections discussed in sub-chapter 2.1.2

(7) Landslide inventory

A landslide inventory is a detailed register of the distribution and characteristics of past landslides. Historical disaster data (location, type, damage scale, response, etc.) and the subsequent landslide inventory preparation are important for generating the landslide hazard/susceptibility map. This map exercise and the subsequent risk assessment process are based on statistical methods. A landslide inventory can be built using past records and high-resolution satellite imagery, such as Google Earth or Sentinel.

Currently there are no comprehensive landslide inventory databases covering the case study area. In the absence of these detailed landslide inventories, an inventory covering the study areas was created using free access satellite images, such as those from Google Earth. This additional landslide inventory data helps generate better landslide susceptibility prediction accuracy.

2.1.2. Rainfall data derived from climate projection scenarios

Hydro-meteorological data consists of a precipitation (mainly rainfall) time-series derived from historical climate data and future climate projection scenarios as discussed in this section.

A changing climate may lead to changes in the frequency, intensity, spatial extent, duration, and timing of weather and climate extremes, and can result in unprecedented extremes (Seneviratne et al., 2012). Weather or climate events that are not extreme in a strict statistical sense can cause extreme conditions or impacts either by crossing a critical threshold in a social, ecological, or physical system, or by occurring simultaneously with other events. Some climate extremes may not be the result of one event but an accumulation of multiple single events (Seneviratne et al., 2012). Under the changing climate, it is indispensable to attribute whether a rise in extreme events is a normal recurrence or it indicates the changing profile of weather-related events. There are three types of challenges. First, to understand and attribute the relative contribution of global warming for triggering extreme hydrological events on a given scale, intensity and frequency. Second, to predict by how much the global warming induced climate change is going to escalate the extreme hydrological events in future. Third, and most importantly, how to correctly predict the abnormal changes in hydrological events at a given spatial scale and use that information for decision making by minimizing uncertainty.

This section introduces the development of climate scenarios and explains its application for landslide risk assessment and mapping. One of the critical challenges for scenario development is to downscale global and regional scale projections into a watershed scale. This process is fraught with high uncertainty. Therefore, utilization of downscaled results at the local or watershed scale is far from straightforward. It needs to adopt a cautious approach and treat the results by contrasting them with the local context. A good understanding of observed data, climate simulations and projections mechanisms and uncertainties is essential to develop realistic scenarios and properly assess the risks in each local context. The whole process should be designed such that decision makers will be able to understand, interpret and use the results from climate simulation and projections and then develop realistic scenarios for planning, mitigation measure design and implementation.

Climate projections are the widely used datasets to help understand climate extremes and their probability of occurrence in the future. The construction, assessment, and communication of climate change projections, including regional projections for extremes, can be drawn from four sources (Seneviratne et al., 2012; Christensen et al., 2007; Knutti et al., 2010), including global climate models (GCMs), downscaling of GCM simulations and physical understanding of the processes governing regional responses and recent historical climate change.

The process of climate impact modeling for identification of extreme events at the watershed or local scale consists of six methodological steps as shown in **Figure 2.7**.

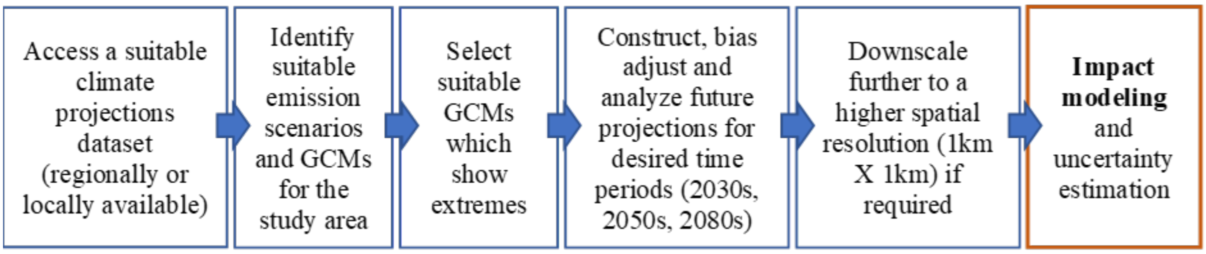

Figure 2.7 Impact modeling for assessing risk from extreme landslides at the watershed scale using downscaled GCMs

2.1.3. Available global/regional circulation models and their selection for developing realistic scenarios

Global circulation models (GCMs) were the main source of globally available regional information on the range of possible future climates including extremes (Christensen et al., 2007) during the Fourth Assessment Report (AR4) of Intergovernmental Panel on Climate Change (IPCC). The IPCC AR4 concluded that extreme events statistics for the present day climate, especially temperature, could be well simulated by current GCMs at the global scale, but simulating precipitation extremes are less robust (Randall et al., 2007). With spatial resolution improvement as well as their complexity, GCMs can be useful for investigating smaller-scale features, including changes in extreme weather events. However, while projecting climate and weather extremes, not all atmospheric phenomena are potentially of relevance and can be realistically or explicitly simulated (Seneviratne et al., 2012). Nevertheless, the requirement for projections of extreme events has provided motivation for the development of regionalization or downscaling techniques (Carter et al., 2007). These have been specifically developed for the study of regional and local-scale climate change, to simulate weather and climate at finer spatial resolutions than is possible with GCMs – a step that is particularly relevant for many extremes given their spatial scale. Studies have indicated that climate models are fundamental tools for simulating and understanding regional and local-scale climate, as well as understanding impacts on the environmental system (Wang et al., 2013; Ahmadalipour et al., 2015). These models use quantitative methods to simulate the interactions of the atmosphere, oceans, land surface, and ice and provide plausible estimates of future climate change.

The Coupled Model Inter-comparison Project Phase 5 (CMIP5) is the latest group of datasets available with simulation from the new generation of GCMs (Rupp et al., 2013). There are more than 40 GCMs in the CMIP5 archive with different spatial resolution that were developed by various meteorological organizations and agencies. In the Fifth Assessment Report (AR5) of IPCC, climate simulations have been carried out for the 21st century according to representative concentration pathways (RCPs) based on four greenhouse gas (GHG) concentration trajectories (Demirel and Moradkhani, 2016).

RCPs are the latest generation of scenarios that provide climate model input. These pathways describe different climate futures, all of which are considered possible depending on the volume of greenhouse gases emitted in the years to come. There are four pathways: RCP8.5 (high emissions), RCP6.0 (intermediate emissions), RCP4.5 (intermediate emissions) and RCP2.6 (low emissions). The goal of working with scenarios is not to predict the future but to better understand uncertainties and alternative futures, in order to consider how robust different decisions or options may be under a wide range of possible futures.

A number of research groups around the globe are engaged in evolving models to simulate the current climate and its future progression under several GHG and aerosol scenarios (Buser et al., 2009) by means of downscaling GCMs. The NASA Earth Exchange (NEX) Downscaled Climate Projections (NEX-DCP30) dataset is the only globally available downscaled climate scenarios that are derived from the GCM runs conducted under the CMIP5 (Taylor et al. 2012) and across the four GHG emission scenarios known as RCPs (Meinshausen et al. 2011) developed for IPCC AR5. The dataset includes downscaled projections from 21 models, as well as ensemble statistics calculated for each RCP from all model runs available. The purpose of these datasets is to provide a set of high resolution, bias-corrected climate change projections that can be used to evaluate climate change impacts on processes that are sensitive to finer-scale climate gradients and the effects of local topography on climate conditions. Each of the climate projections includes monthly averaged maximum temperature, minimum temperature, and precipitation for the years from 1950 through 2005 (retrospective run) and from 2006 to 2099 (prospective run).

The bias correction and spatial disaggregation (BCSD) approach used in downscaling datasets inherently assumes that the relative spatial patterns in temperature and precipitation observed from 1950 through 2005 will remain constant under future climate change. Other than the higher spatial resolution and bias correction, this dataset does not add information beyond what is contained in the original CMIP5 scenarios and preserves the frequency of periods of anomalously high and low temperature or precipitation (i.e., extreme events) within each individual CMIP5 scenario. The purpose of these datasets is to provide a set of global, high resolution, bias-corrected climate change projections that can be used to evaluate climate change impacts on processes that are sensitive to finer-scale climate gradients and the effects of local topography on climate conditions. The datasets also assist the science community in understanding the impacts of climate change at regional, national and local levels, in addition to enhancing public understanding of possible consequences. **Table 2.1** summarizes the data field description for the NASA Earth Exchange-Global Daily Downscaled Projections (NEX-GDDP).

2.1.4. Datasets for predicting future climate scenarios

Historical as well as future climate projection data is needed for the analysis. There are several sources of globally and regionally available historical meteorological datasets. CHIRPS precipitation data from Climate Hazard Group (CHG), with 5x5 km2 resolution, is available from 1981 to date. APHRODITE project precipitation data from RIHN/MRI/JMA, with 25x25km2 resolution, is available from 1951 to 2007. For temperature, ERA5 reanalysis temperature data (https://cds.climate.copernicus.eu), is available from 1950. In addition, in-situ observed meteorological data (rain gauge, temperature data) over a longer period is also needed for result verifications and GCM bias corrections.

After selecting the climate projection data, a thorough review is suggested to acquire/access future climate change data with acceptable horizontal resolution to assess the impacts on future climate relevant sectors in target countries. The NEX models (CMIP5 models) that has future climate change scenarios from 21 GMCs under two emission scenarios (RCP 4.5 and 8.5) with 25x25 km2 resolution provides a good database for starting the analyses, in particular the regional analysis.

Table 2.1 Field Description for NEX-GDDP

CMIP5 models included	21 GCMs ACCESS1-0, CSIRO-MK3-6-0, MIROC-ESM, BCC-CSM CM3, MIROC-ESM-CHEM, BNU-ESM, GFDL-ESM2G CanESM2, GFDL-ESM2M, MPI-ESM-LR, CCSM4, INM ESM-MR, CESM1-BGC, IPSL-CM5A-LR, MRI-CGCM CM5, IPSL-CM5A-MR, NorESM1-M
RCP scenarios	RCP 4.5 and RCP 8.5
Temporal resolution	Daily from 1950-01-01 to 2100-12-31 From 1950 through 2005 (“retrospective run”) and From 2006 to 2100 (“prospective run”)
Spatial resolution	0.25 degrees x 0.25 degrees
Climate variables	Precipitation, maximum and minimum temperature
Dataset projection and datum	Geographic, WGS84
Data access	https://www.nccs.nasa.gov/services/data-collections/land-based-products/nex-gddp

All GCMs of the CMIP5 are not applicable for all regions of the globe. Based on the region of interest, GCMs should be selected from those available under CMIP5. For example, in the case of the RBP in Myanmar, a selection of suitable GCMs for the target areas was carried out based on published reports and journal papers such as “Evaluating the performance of the latest climate models over Southeast Asia” published by CSIRO, Australia for the Asian Development Bank (ADB) (Hernaman et al., 2017). The report was used to identify and select suitable models for the Southeast Asia region, including Myanmar. This literature identified a subset of CMIP5 models based on a set of metrics that avoided least realistic models but included models to capture the maximum possible range of change with satisfactory performance across all metrics. On the basis of these studies the following GCMs were selected for the target areas as shown in **Table 2.2**.

Table 2.2 Target area GCMs Considered for the present study

Target area	Selected GCM
Myanmar	bcc-csm1-1, BNU-ESM, CanESM2, CESM1-BGC, CSIRO-Mk3-6-0, GFDL-CM3, GFDL-ESM2G, GFDL-ESM2M, IPSL-CM5A-MR, MPI-ESM-LR, MPI-ESM-MR

The present study focuses on identifying extreme events in the future with an aim to understand the possible maximum hazardous level for the target areas. It is therefore logical to identify those amongst the 10 models that depict the extreme events in the future in the target areas. In the RBPs, the future scenarios of 2030 (taking an average from 2016-2045), 2050 (taking an average from 2036-2065) and 2080 (taking average from 2066-2095) are generated based on current climate (rainfall and mean temperature from 1976-2005) over the same study area during the wet season. Since landslides are more prominent during the wet (monsoon) season, in this case the period between May – September, this is considered the most suitable time period for selecting GCMs.

A scatter plot is suggested for model identification. The scatter plot involves calculation of the change in annual mean temperature (ΔT) and the percentage of change in annual precipitation (ΔP%) from each of the models (CMIP5) from NEX with RCP4.5 and RCP8.5 emission scenarios. The results are plotted in a scatter plot for Southeast Asia and South Asia that give possible extreme conditions in the region during the 2030s, 2050s and 2080s. The models that are closest to the 5th and 95th percentile of the change of annual mean temperature (ΔT) and percentage change of annual precipitation (ΔP%) during the 2030s, 2050s and 2080s in the two RCPs can be selected. To depict the methodology, **Figure 2.7** shows the skills test scatter plots for identifying suitable GCMs to predict extreme conditions at the Taunggyi Watershed in Myanmar during the 2080s.

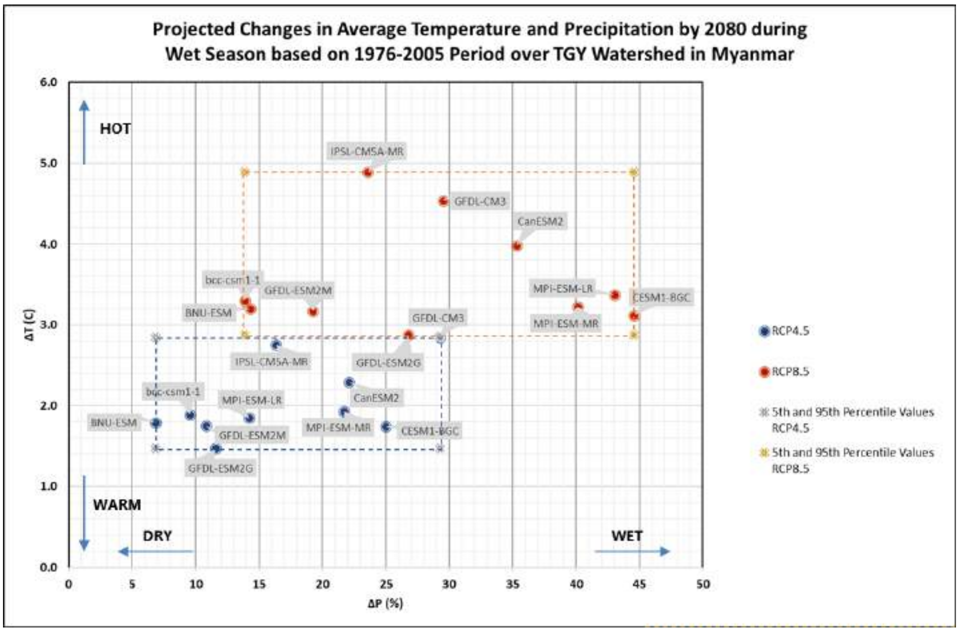

Figure 2.8 Scatter plots for identifying suitable GCMs to predict extreme conditions at the Taunggyi Watershed in Myanmar during the 2080s

As per **Figure 2.8** the CESM1-BGC (wettest) and bcc-csm1-1 (driest) models show extreme conditions (temperature and precipitation) in the Taunggyi Watershed during all time horizons with RCP 4.5 and RCP 8.5 scenarios out of the 10 GCMs.

Table 2.3 shows the summary of selected suitable GCMs that were identified to represent possible extreme conditions for target areas.

Table 2.3 Identification of GCMs showing the highest (wettest) and lowest (driest) extremes in the areas of interest

Target area	Highest extreme (wettest)	Lowest extreme (driest)
Taunggyi watershed	CESM1-BGC	bcc-csm1-1

Since it is obvious that temperature has little effect on rainfall triggering landslides in each watershed size, rainfall is the only considered climatological variable.

The advantages of using the skills test to identify extreme GCMS are:

- Different climate variables from different models (or sets of models) are not mixed. Mixing may lead to values having internal inconsistency and may not be physically plausible.
- The test ensures all information and data is placed in the context of the used emissions scenarios (RCP 4.5 is a medium scale emission scenario, whereas RCP8.5 is a strong mitigation scenario).
- Baseline periods are of sufficient duration to include a range of climate variations and encompass the same number of years as the future periods.
- The GCM biases were handled by converting results to changes relative to a baseline period or by using a bias correction method such as BCSD method considered in this study (ADB, 2017)
- It seeks the optimal balance between ensuring that the selected GCMs represent changes in average and extreme climatic conditions well but at the same time must have reasonable adaptability in simulating the past climate, with a focus on monsoon dynamics.

There are also some disadvantages of the skills test approach of GCM selection:

- Scale of the application can be an issue. During the first selection step, projected changes are averaged over the entire area. This may dilute the spatial variation in projected changes (A potential solution for that is to divide the study area into multiple parts and apply the selection approach to each part independently).
- It envelopes changes in means during the selection approach. This may result in a reduction in the range of change projections in climatic extremes in the ensemble.
- Downscaling to construct a higher resolution (1km x 1km) climate surface

Since the NEX dataset resolution is coarse (25x25km2), it might prevent a detailed analysis of climate change at national, and in particular, local scales such as at RBP sites. A comprehensive analysis of local climate change impacts and future planning requires local, high-resolution climate variables that cannot be obtained directly from coarse resolution projections (Komurcu et al., 2018). Therefore, it is important to include a downscaling methodology for generating high resolution (1kmx1km) datasets for further impact studies in the target areas.

Since it is difficult to find a strong relationship between precipitation and elevation to build a nonlinear or circular function, a straight univariate bilinear resampling method is proposed for resampling of 25kmx25km resolution precipitation data into a 1kmx1km resolution grid. The APHRODITE dataset can be used as the reference surface to resample precipitation surface. This resampling process can generate approximate patterns as per the reference data surface and it does not disturb the pattern of the original GCM. Downscaling to 1kmx1km resolution was carried out in selected GCMs using the above process in RBPs that represent possible extreme conditions. The downscaled 1kmx1km resolution datasets then were used for developing future climate projections and analysis of rainfall hotspots for target areas.

2.1.5. Methodology for impact modelling

Identification of hotspots and intensity of associated hazards is done through impact modeling that is carried out after a selection of suitable GCMs and construction of the current climate using historical data from satellite-derived and in-situ datasets. Climate analysis results in Taunggyi Watershed are described below.

2.1.6. Developing rainfall intensity climate change projections

Analyses of wet season total rainfall changes in Taunggyi Watershed in the 2030s, 2050s and 2080s with respect to the baseline (1976-2005) under RCP 4.5 and 8.5 emission scenarios were derived for CESM1-BGC (wettest-highest extreme) and bcc-csm1-1 (driest-lowest extreme) GCMs. The following figures show the wet season average precipitation changes for RCP 4.5 and RCP 8.5 respectively.

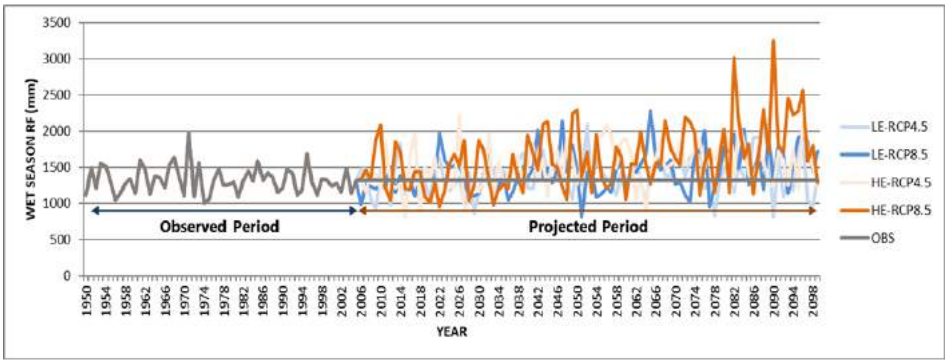

Figure 2.9 Historical and projected variability of wet season rainfall – Taunggyi Watershed

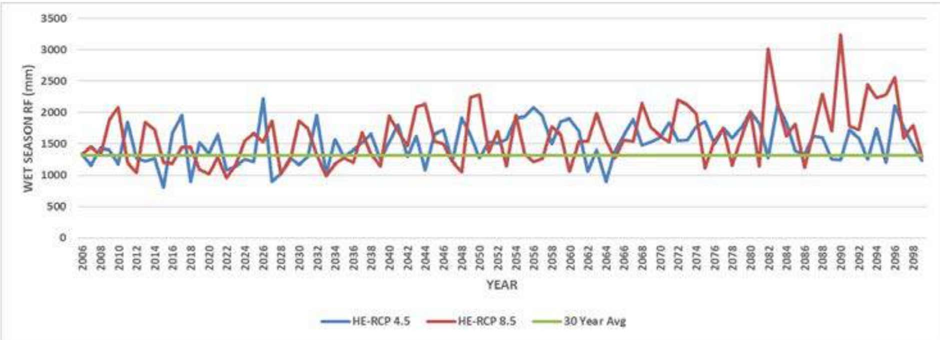

Figure 2.10 Projected variability of wet season rainfall with respect to climatology for wettest-highest extreme GCM – Taunggyi Watershed

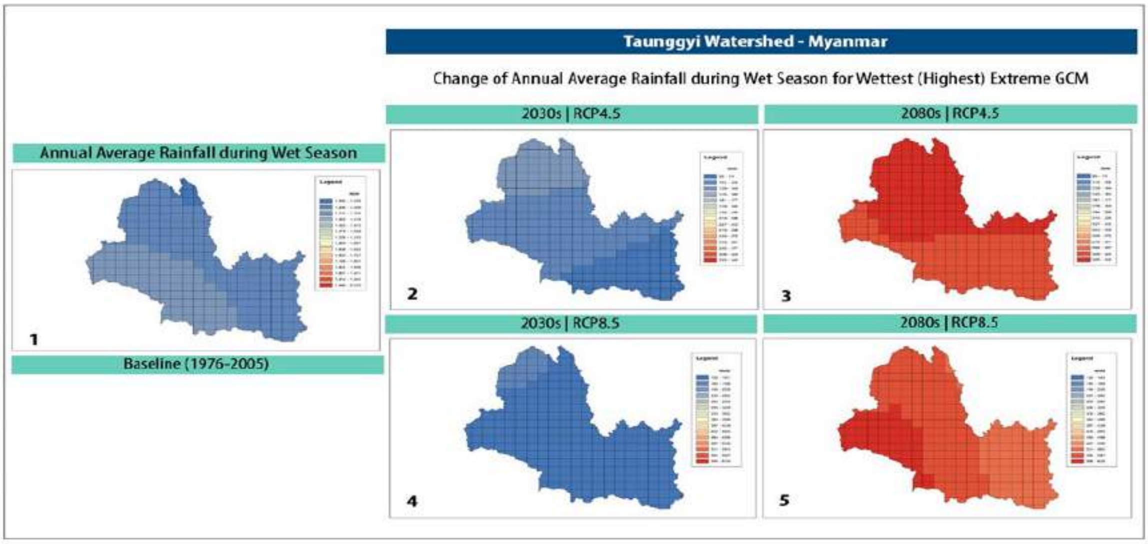

Figure 2.11 Average rainfall during wet season (climatology-1976-2005) (2) Change in annual average rainfall during wet season by 2030, wettest-highest extreme GCM, RCP4.5. (3) Change in annual average rainfall during wet season by 2080, wettest-highest extreme GCM

The below table depicts the likely amount of rainfall change in millimeters (mm) with respect to the baseline period for each time horizon and emission scenario for wettest-highest extreme GCM.

Table 2.4 Likely amount of rainfall change for each time horizon

Time horizon	RCP 4.5	RCP 8.5	Remarks
2030s	87	115	Rainfall is likely to increase 67% and 70% for RCP 4.5 and RCP 8.5 respectively in the future
2050s	237	242	
2080s	290	543	

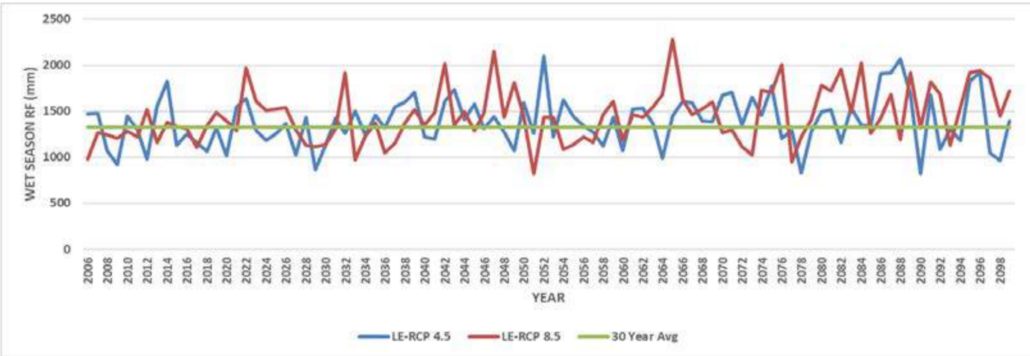

Figure 2.12 Projected variability of wet season rainfall with respect to climatology for driest-lowest extreme GCM – Taunggyi Watershed

The table below depicts the likely amount of rainfall change in mm with respect to the baseline period for each time horizon and emission scenario for lowest extreme GCM.

Table 2.5 Likely amount of rainfall change (in mm) for each time horizon

Time horizon	RCP 4.5	RCP 8.5	Remarks
2030s	20	64	Rainfall is likely to increase 67% for RCP 4.5 toward the distant future and is likely to decrease 70% for RCP 8.5 toward the distant future
2050s	87	121	
2080s	145	203	

The results indicate the wettest GCM in medium and high emission scenarios shows a considerable spatial variability with projected wet season rainfall gradual increase in the three-time horizons. In the wet season, average rainfall is also projected to increase by 67 percent and 70 percent for both emission scenarios toward the distant future. This increase is gradual over all future time horizons. The driest GCM also shows a similar trend of an increase in wet season rainfall by the 2080s for both emission scenarios. Thus, the results likely indicate that landslide hazards may be common in the hilly areas in the future in the Taunggyi watershed in Myanmar.

2.2. Conclusion

- The wettest (highest extreme) GCM for each target area clearly shows an increasing trend in wet season rainfall in the future for the respective target watershed.
- The driest (lowest extreme) GCM also shows an increasing rainfall trend in Taunggyi watersheds during the wet season.
- Both intermediate (RCP 4.5) and high (RCP 8.5) emission scenarios have a similar pattern of rainfall change in the future.
- It is recommended to run an impact model for both the highest and lowest extreme GCMs as well as both medium and high emission scenarios to understand the full range of variability in the future. Climate projections are not predictions of the future, but instead provide a range of possible future climate. As such, projection values should be used to guide thinking in impact assessments and planning, and users should include flexibility in their planning and adopt an adaptive management approach to allow for change as more information becomes available through appropriate observational-based monitoring, scientific research, and evaluation.

2.3. Understanding the uncertainty

There are two factors to consider when dealing with uncertainties in climate modeling. One is GCM uncertainty – uncertainty in climate system response and u natural variability. The other is uncertainty in future emissions and future concentration of greenhouse gases (GHGs). GCM uncertainty can be addressed using projections from a range of GCMs and an ensemble of GCM projections with different initial conditions. Uncertainty in future emissions and future concentrations can be addressed using a number of carbon cycle and atmospheric chemistry models, in addition to climate models under a range of emission scenarios such as RCP 4.5 and 8.5.

Even after selecting the best available approaches or strategies for climate modelling and projections, they are not necessarily complete or meant to be adopted directly for decision making. As such, climate projections are not predictions of the future. Instead, the projections provide a range of possible future climate. The projection values should be used to guide thinking in impact assessments and planning, and users should include flexibility in their planning and adopt an adaptive management approach to allow for change as more information becomes available through appropriate observational-based monitoring, scientific research, and evaluation.

2.1.3 Landslide Susceptibility Map Zoning using Weight of Evidence

Calculation of each particular predictive hazard variable involves assigning a positive weight (W+), when the event occurs and a negative weight (W-), when the event does not occur. The weights are measures of correlation between evidence (predictive variable) and event, making them easy to interpret in relation to empirical observation. Formulation is based on density functions. Weights (Wi) of each cell (ith pixel) are determined by the equation:

$$W_i = \sum_{j=1}^{n} W_j^k$$

Where Wj is a parameter of the jth class and wk signifies positive and negative weight values. Controlling landslide factors can be mapped with this method. The weights can be used to produce a contrast value (C) for the specific susceptibility variable.

$$C = W^+ - W^-$$

The difference between weights (C) provides a measure of strength of correlation between the analyzed variable and the landslide.

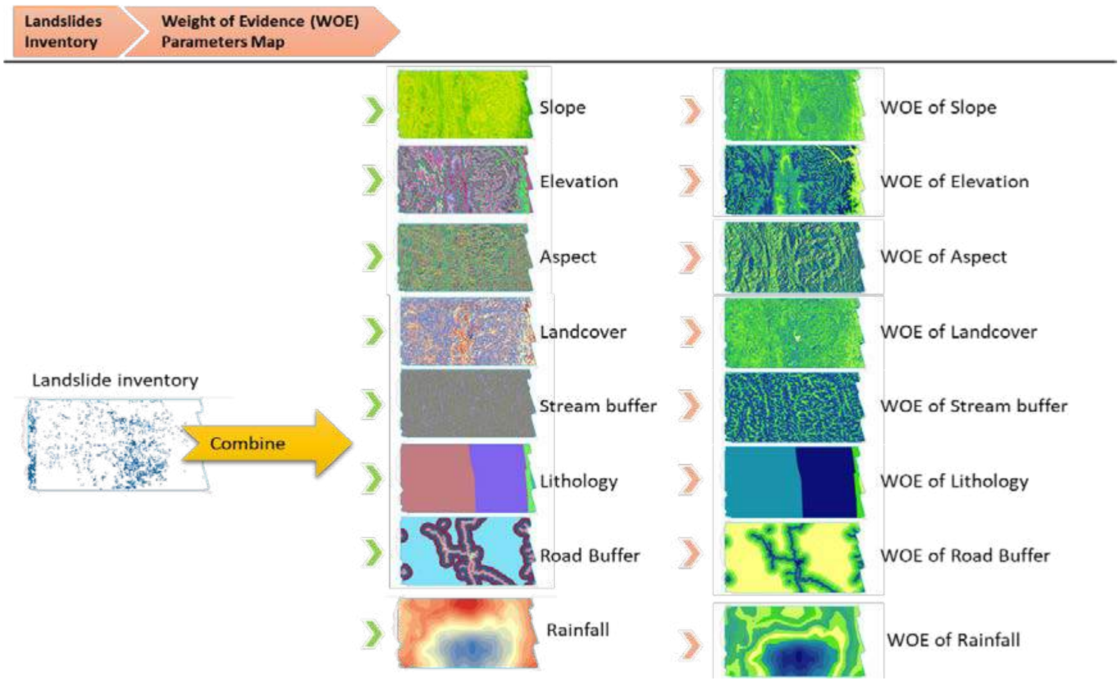

Figure 2.13 Landslide susceptibility assessment using WOE (where rainfall data was derived from future climate scenarios)

Susceptibility zoning uses GIS to overlay the weight of evidence (WOE) parameter maps. The overlaid map is first divided into approximately 255 classes (the more classes the better), at equal intervals from high to low WOE. These classes are then analyzed with a landslide occurrence using the raster analysis.

Based on the sorted classes, susceptibility zones are defined as follows:

50% of landslide occurrence is classified as a very high zone
20% of landslide occurrence is classified as a high zone
15% of landslide occurrence is classified as a medium/moderate zone
10% of landslide occurrence is classified as a low zone
5% of landslide occurrence is classified as a very low zone

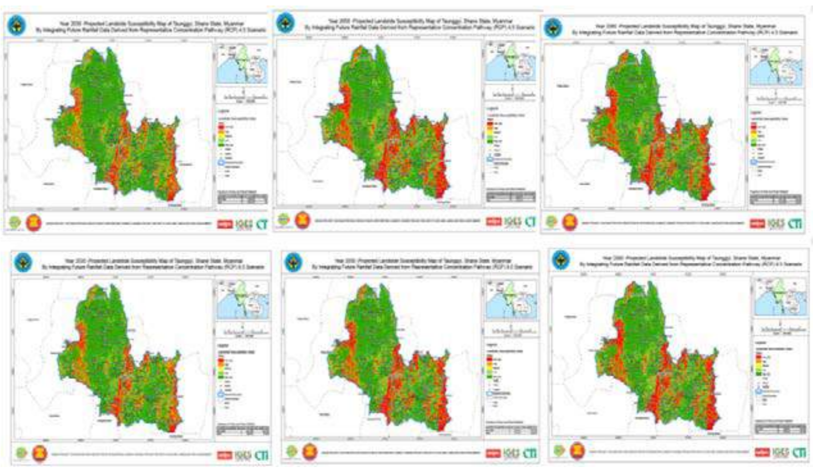

Figure 2.14 Taunggyi landslide susceptibility with results from two different future climate scenarios (RCP 4.5 and RCP 8.5)

A geometry calculation was done in the Geographic Information Systems (GIS) environment to quantify the total area of landslide susceptibility. **Figure 2.15** shows the increases in areas in the high and very high landslide susceptibility categories.

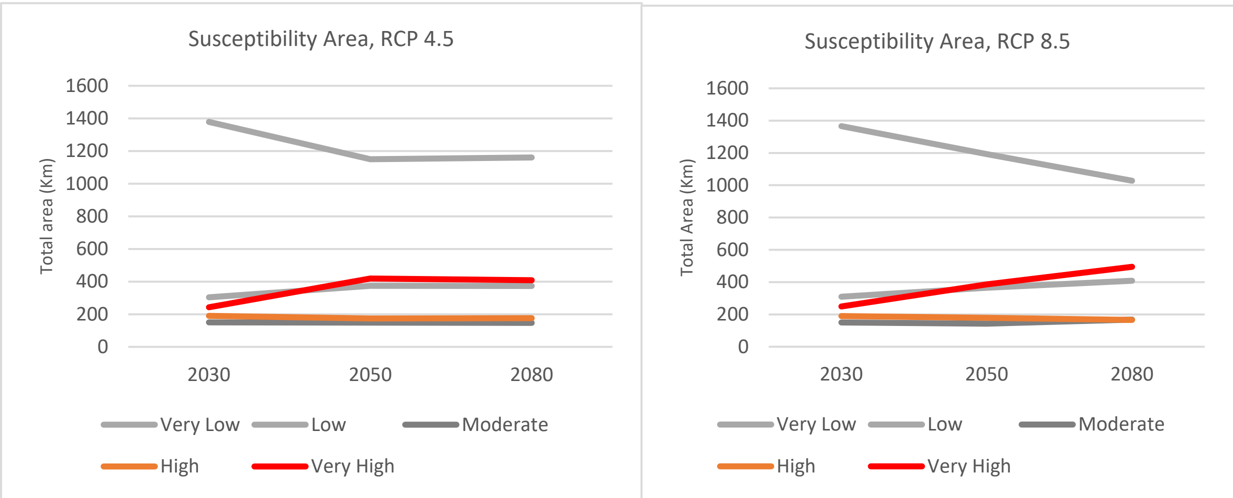

Figure 2.15 Area trends in different landslide susceptibility categories in the Taunggyi RBP in two different future climate scenarios (RCP 4.5 and RCP 8.5)

Table 2.6 Total area of landslide susceptibility in Taunggyi, RCP 4.5

Susceptibility Area	RCP 4.5 (Km^2)		
	2030s	2050s	2080s
Very low	1378,59	1149,93	1160,84
Low	303,70	374,09	372,81
Moderate	150,23	148,42	146,97
High	190,06	173,96	175,84
Very high	242,69	418,88	408,81
Grand Total	2265,27	2265,27	2265,27

Table 2.7 Total area of landslide susceptibility in Taunggyi, RCP 8.5

Susceptibility Area	RCP 8.5 (Km^2)		
	2030s	2050s	2080s
Very low	1365,82	1192,44	1027,77
Low	309,65	364,87	408,58
Moderate	150,63	142,78	167,99
High	189,84	178,79	166,04
Very high	249,33	386,39	494,89
Grand Total	2265,27	2265,27	2265,27

Results show a trend of increases in areas susceptible to landslides in the 2030s, 2050s and 2080s for both IPCC scenarios of RCP 4.5 and RCP 8.5.

2.4. Exposure assessment

One of the main steps in risk assessment is to evaluate the element at-risk when exposed to different hazards. This is called an exposure assessment. As defined by UNISDR (2004), exposure indicates the degree to which the elements at risk are exposed to a particular hazard. The exposure can also be defined as the total number/value of the element at risk. Exposure is the total value of elements at risk. It is expressed as the number of human lives and the number/value of the properties or assets that can potentially be affected by hazards. An exposure assessment is an intermediate stage of the risk assessment that evaluates the element at-risk to different hazards.

The exposure assessment in this case study includes a quantification of the number of households (sampling) located in hazard-prone areas. The analysis is carried out for households that have the potential to be significantly affected. Sampling data for a total of 200 households was collected from the field survey in 2019, but the analysis focuses on 171 households that are located within the Taunggyi watershed area. The spatial household information/attributes are overlaid with landslide susceptibility maps using GIS tools. The following flowchart depicts the process of spatial overlay between landslide susceptibility maps and household data sampling.

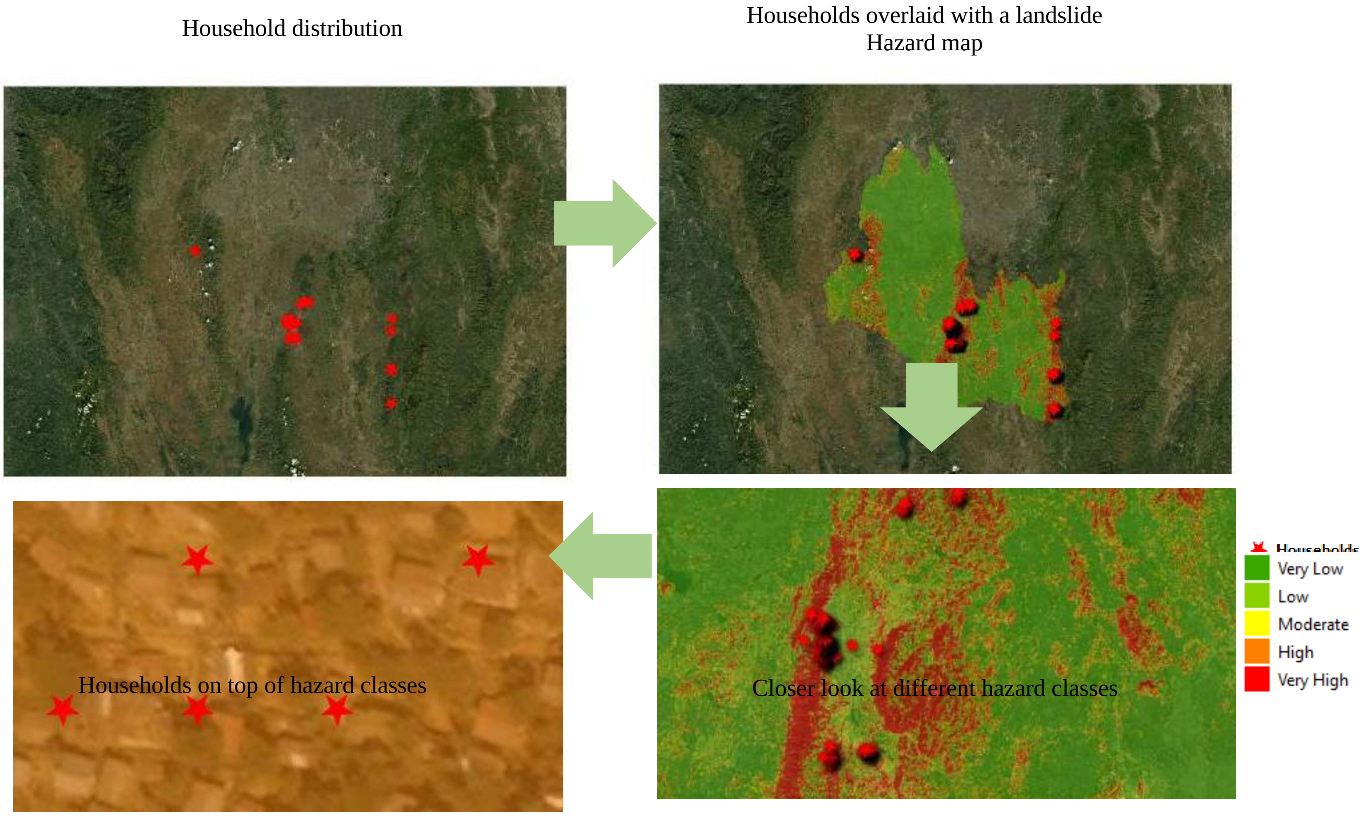

Figure 2.16 Illustrations of exposure (spatially overlaid between landslide susceptibility maps and household)

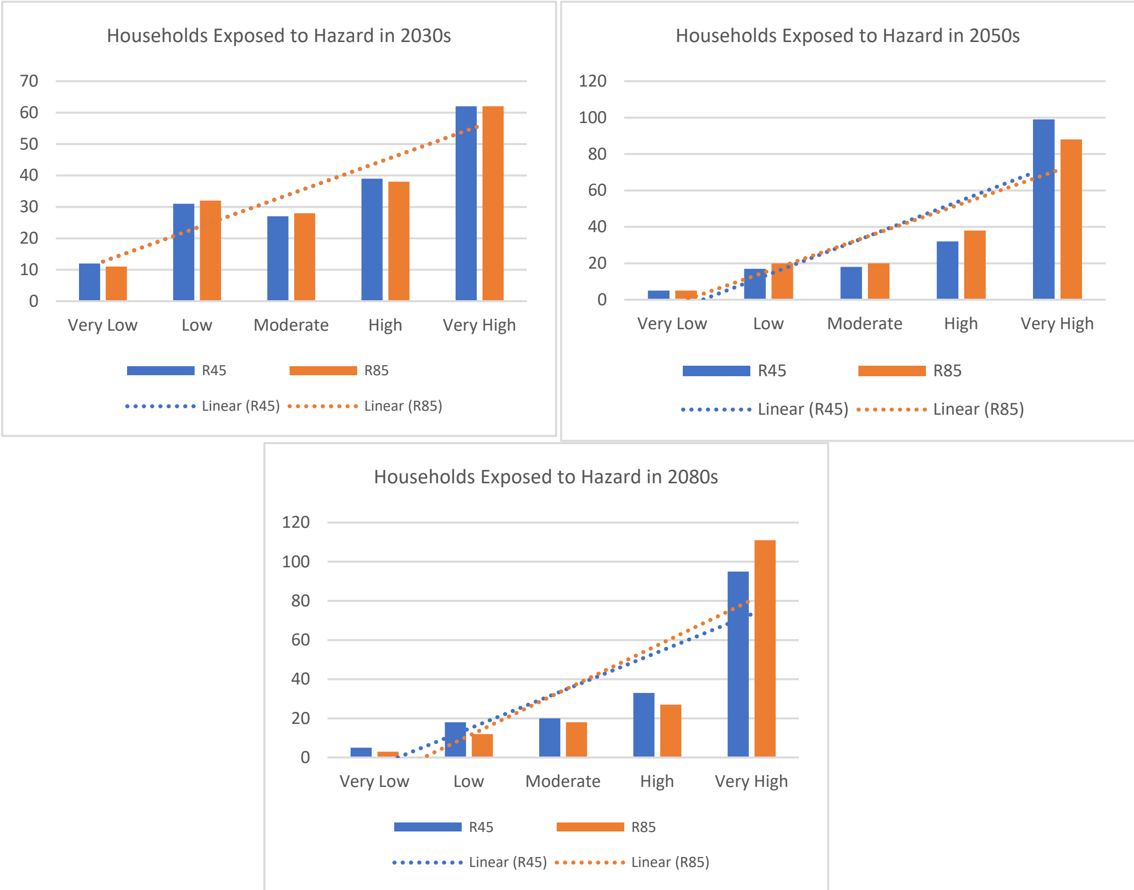

Figure 2.17 Distribution of households exposed to high and very high landslide hazard categories in Taunggyi, Myanmar

Figure 2.18 shows results from households exposed to different landslide categories made up of five classes: very low, low, moderate, high and very high. The majority of households that fell under *high* and *very high* categories showed a trend in increases for both IPCC scenarios of RCP 4.5 and RCP 8.5 throughout the three projected time periods of the 2030s, 2050s and 2080s.

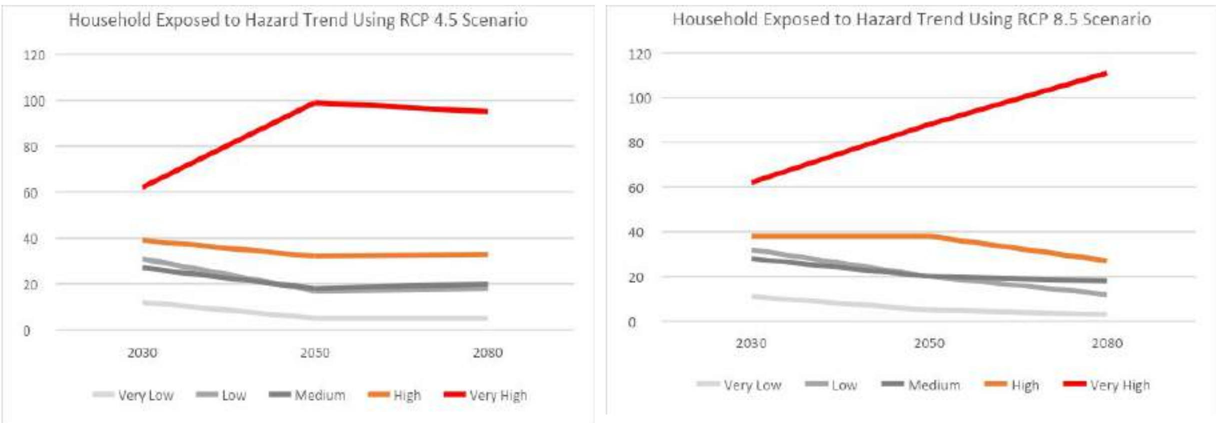

Figure 2.18 Trends in number of households exposed to different landslide susceptibility categories in Taunggyi RBP, Myanmar for the three projected times of the 2030s, 2050s and 2080s

Hazard Class	RCP 4.5			RCP 8.5		
	2030s	2050s	2080s	2030s	2050s	2080s
Very low	12	5	5	11	5	3
Low	31	17	18	32	20	12
Medium	27	18	20	28	20	18
High	39	32	33	38	38	27
Very high	62	99	95	62	88	111
Grand Total	171	171	171	171	171	171

Table 2.8 Trends in number of households exposed to different landslide susceptibility categories in Taunggyi RBP, Myanmar for the three projected times of the 2030s, 2050s and 2080s

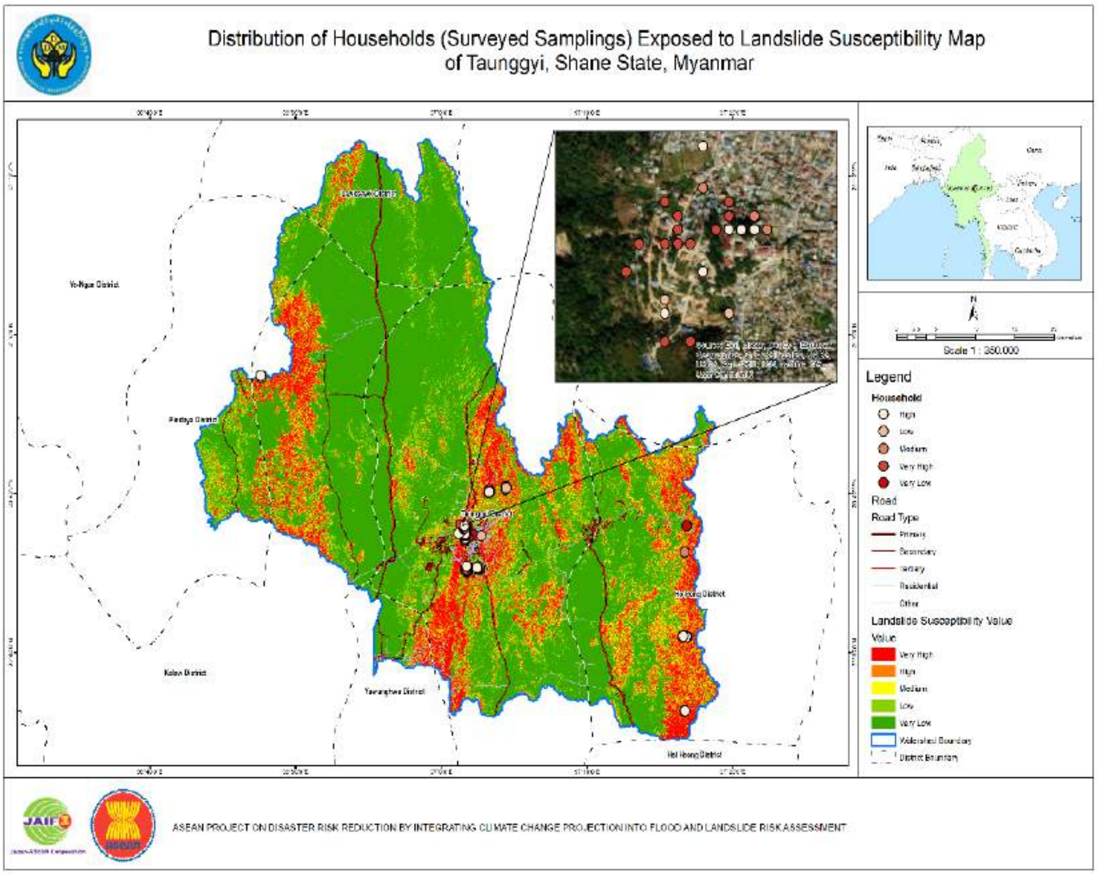

Figure 2.19 Spatial distribution of surveyed households exposed to landslide susceptibility zones in Taunggyi RBP, Shane State, Myanmar

2.4.2. Exposure Assessment limitations

The household data collected for this study was limited. It was analyzed in a Geographic Information Systems (GIS) environment and presented at the household level as point shapefile (GIS format). It is recommended that more details and comprehensive household data covering the study area are collected and included in future analyses.

2.5. Vulnerability and capacity assessments

2.5.2. Vulnerability Assessment

The vulnerability assessment results presented here are derived from the methodologies outlined in text of the landslide guidelines.

Landslide vulnerably scoring (LVS) is used for assessing household landslide vulnerability. It is a qualitative method of assessing individual household landslide vulnerability wherein scores are assigned to an individual indicator based on the value the indicator takes and how that value corresponds to the overall vulnerability that is constructed as a range (i.e., 0 means no vulnerability and 1 means high vulnerability).

***Assigning scores*: ** The basis for LVS is published literature (e.g., for below poverty line, etc.) when possible and expert judgements. For assigning the ratings, a structural elements resistance factor is used. However, due to lack of resistance factors for the location-specific conditions, literature available elsewhere was used to decide gradient of ratings allocated to different structural elements (for example, a reinforced concrete (RC) building is considered to have a high resistance factor compared to stone masonry structures, framed structures have higher resistance than load-bearing structures, etc.). Similarly, recent construction (less than 10 years old) can be considered to have higher resistance than older construction. Scoring mostly follows a binary classification wherever possible to simplify the vulnerability assessment and for ease in understanding results. If more resolution is necessary for scoring, ternary and quaternary scores are also assigned.

Data normalization: Since indicators can have different ratings based on different units of measurement (e.g. km, years etc.), a linear normalization method has been employed to bring all indicators to a 0-1 scale so that the values can be combined within a category.

The formula for normalizing the indicator values is given as:

Normalized value

$$z_i = \frac{x_i - T_{\min}(x)}{T_{\max}(x) - T_{\min}(x)}$$

Where: x_i is the value of the indicator

T_{min} is the minimum threshold value of the indicator xi
T_{max} is the maximum threshold value of the indicator xi.

Mutual dependencies and indicator hierarchy: Indicators have a mutual dependency/hierarchy. For example, RC construction that is recent but has a shallow foundation or does not satisfy basic conditions of anchoring to bedrock could be more vulnerable to damage than other types of framed structures such as bamboo that are anchored to bedrock. These types of interdependencies, however, were not considered for this preliminary analysis, and their results will have to be updated for such dependencies at the next stage.

Weightages: Indicators can take on relative weightings depending on the importance they play in the final vulnerability. For example, if structural vulnerability plays a larger role than social vulnerability due to its physical location or the type of house, structural vulnerability can be given higher weightage in the overall vulnerability. However, such weightages need careful consideration based on evidence (empirical studies). Since no such studies were available for the study location, all vulnerabilities were considered equal.

Proxy indicators were derived for higher relevance to the vulnerability assessment. For example, the distance to a health care center is converted into minimum response time (MRT) equivalent distance (MED) to imply that the difference between the actual distance and the MRD results in higher vulnerability. Similarly, the number of people in the household is converted into household residence time (HRT) to imply the higher the HRT, the higher the vulnerability.

Table 2.9 Priority socio-economic sensitivity indicators

Indicator	Description
Family without educated members	Counts all households without an educated person. This household type has a landslide vulnerably score (LVS) rating (landslide risk sensitivity).
Vulnerable population	Counts all households with a woman, child, and/or an elder older than 60 years. A household that satisfies at least one of these conditions is given an LVS rating of 1, two conditions LVS 2, and 3 conditions LVS 3. This data is then normalized to a 0-1 scale to combine with other indicators.
Female headed household	Counts households that do not have a living male elder. Given an LVS of 1.
Differently abled	Counts households with a physically disabled family member. Given an LVS of 1. This is in addition to gender and age considerations (for example a household with a disabled female will get two LVS values).
Poverty	Counts the monthly poverty income line. Households below the income poverty line are given an LVS of 1.
Access to health	Counts the household’s distance to a health center. Households beyond a 4.5 km radius from the health center are treated as sensitive, with an LVS of 1.
Home vacant time (HVT)	Counts amount of time during the day a household is vacant. Those with less vacant time are considered the most sensitive. Vacant hour values are linear and are given to fall within the LVS range of 0-1.
Rate of service interruption	Counts the average rate of service (such as water, electricity, etc.) interruption (in percentage) with linear values and is given an LVS range of 0-1.
Interruption duration	Counts number of days of interruption (of water, electricity, etc.) with linear values, and is given an LVS range of 0-1.

Table 2.10 Priority physical sensitivity indicators

Indicator	Description
Land slope	Counts households located on a slope of greater than 15%. These are considered sensitive and are given an LVS of 1.
Living floor	Counts households living on the ground floor. This household type is considered sensitive (in accordance with earthquake literature), and given an LVS of 1.
Building age	Counts buildings more than 10 years old, given an LVS of 1.
Architectural approval	Counts buildings without architectural/formal approval, given an LVS of 1.
Foundation type	Counts buildings that used clay aggregates or rubble in construction, given an LVS of 1.
Bedrock anchoring	Counts buildings with foundations reaching or anchored in bedrock and are given an LVS of 0 (not sensitive).
Nature of walls	Counts load bearing wall structures, and given an LVS of 1.
Damage susceptibility rating	Self-assessed damage susceptibility ratings ranging between 1-10 are linear, normalized to LVS values.

2.6. Capacity Assessment

Capacity is a combination of the strengths and resources that exist within a household, community, group, or organization that can reduce the level of risk or disaster impact. A capacity assessment identifies strengths and resources available to individuals, households and communities to cope, defend, prevent, prepare, reduce risk, or recover quickly from disaster. For this study, six capacity assessment indicators were used, as shown in **Table 2.11** below.

Table 2.11 Capacity indicators

Indicator	Description
Disaster risk management participation	Counts households that have reported DRM participation, and given an LVS of 0.
Microfinance	Counts households that participate in microfinance programs, and given an LVS of 0.
Landslide discussions	Counts households that discuss landslides, and given an LVS of 0.
Migration readiness	Counts households that report having landslide preparedness measures in place, and given an LVS of 0.
Disaster risk management awareness	Counts households that expressed having disaster risk management awareness measures in place, and given an LVS of 0.
Alternative roads	Counts households that have more than one access road, and given an LVS of 0.

The vulnerability assessment results presented here were derived from the methodology outlined in the main landslide guidelines text. As discussed in the guidelines, the primary data on household socio-economic and demographic details was collected through structured questionnaires. It should be noted that a similar study was also done in Phoukhoun RBP located in Luang Prabang Province of Lao PDR, thus several comparisons were made between these two case study areas.

In Taunggyi RBP, 200 households participated in the structured survey. The data was analyzed using the methodology outlined in the landslide guidelines. The structured questionnaire data was extracted according to the sensitivity and capacity indicators presented in **Tables 2.9-2.11**.

The landslide vulnerability (sensitivity and capacity) values were overlaid with the landslide susceptibility values to identify the spatial distribution of sensitivity and capacity in various landslide susceptibility zones. Please note that landslide susceptibility is a geological feature of the location and is not related to vulnerability. Please refer to the relevant sections of the technical report and guidelines for more information on landslide susceptibility.

Figure 2.20 shows the change in household exposure under different climate change scenarios. It indicates that the number of families living in very high landslide susceptibility zones will increase to 65% of the sampled population under an 8.0 OC scenario by the 2080s. At the same time, the number of people living in very low and low landslide susceptibility zones will decline to 2 and 7% of the sampled population respectively. This indicates the urgency to invest in sound disaster risk reduction measures in areas with high and very high landslide susceptibility.

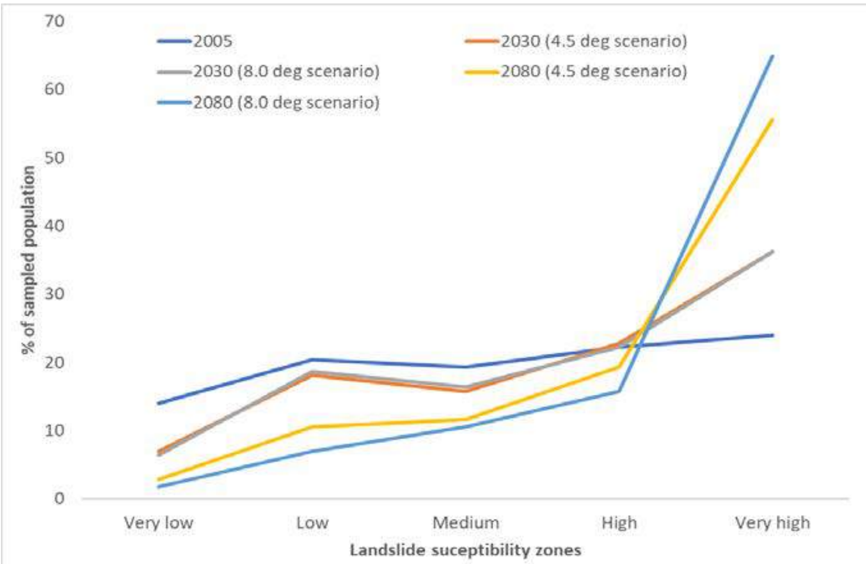

Figure 2.20 Trends in percentage of households living in landslide susceptibility zones under various climate change scenarios

For vulnerability spatial distribution, the vulnerability assessment results for the current period (i.e. 2016-2045, indicated as 2030s) indicated that households had higher sensitivity to landslides than capacity in both the 4.5 and 8.5 degree scenarios (**Figure 2.21**). Secondly, households living in medium landslide susceptibility zones had a marginally lower capacity and sensitivity than families living in other landslide susceptibility zones. This indicates the need to invest in building the capacity and reducing the sensitivity of households living in medium landslide susceptibility zones. This kind of analysis will help operational planning in terms of preparedness, immediate response, and relief measures for various landslide susceptibility zones.

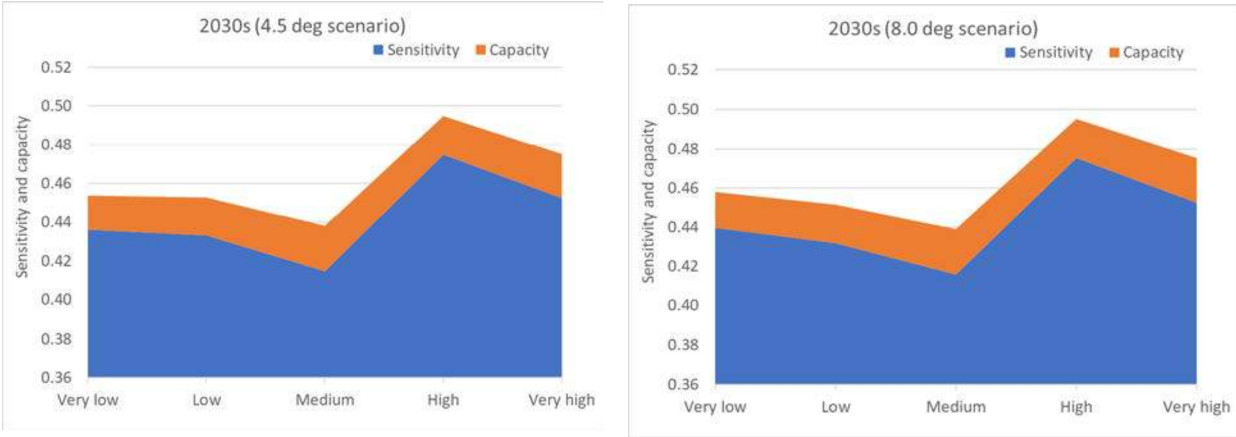

Figure 2.21 Spatial distribution of vulnerability in various landslide susceptibility zones in Myanmar during the 2030s (2016-2045)

The vulnerability assessment results also indicated that female-headed households earned 17 percent less income than male-headed households in the sampled population. This has a marginal impact on family poverty. As a comparison, 19 percent of female-headed households are poor, with only 17 percent of male-headed households poor. A higher incidence of poverty by 2 percentage points in female-headed families indicates that female-headed households are more likely to be affected by economic shocks compared to male-headed households. However, the type of house in which a family is living did not have a bearing on family financial status, which may have to do with the narrow income range of the people and limited choices in building materials used in these locations.

Similarly, there was no difference in income levels between those living on slopes greater than 15 percent that got their house officially approved and those that did not get it approved. Conversely, a negative and insignificant correlation (-0.03) between income and percentage of households living on steep slopes was found in the surveyed locations. Numerical data observation showed that marginally higher-income families lived on steeper slopes (>15 percent). Only 53 percent of households that said they discuss landslides were found to have prepared for landslides. All the households (100 percent) that were found prepared for landslides had discussed landslides. This indicates that a discussion among household members is an important precursor for a household to be prepared for landslides. It cannot be concluded, however, that this preparedness resulted in reduced landslide impacts on these households as no landslides were reported in the recent past in this study location.

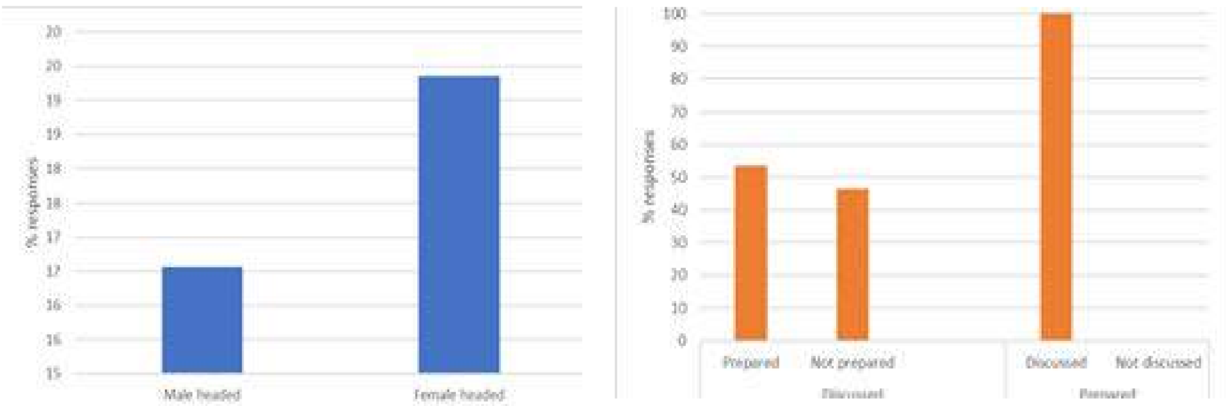

Figure 2.22 Poverty incidence in female headed households in the sampled population at Taunggyi, Myanmar. Right: The positive effect on preparedness due to discussion in the household

The willingness to migrate from disaster-prone areas is an important factor for reducing human exposure. The survey revealed that the willingness to migrate from the slopes to the plains is related to respondent income level (**Figure 2.23**). More households above the poverty line had shown greater willingness to migrate than those below the poverty line. This indicates that the poor are locked in hazard-prone areas and lack sufficient resources to consider other options. The survey also revealed that those living on steeper slopes (>15 percent) showed a higher willingness to migrate than others.

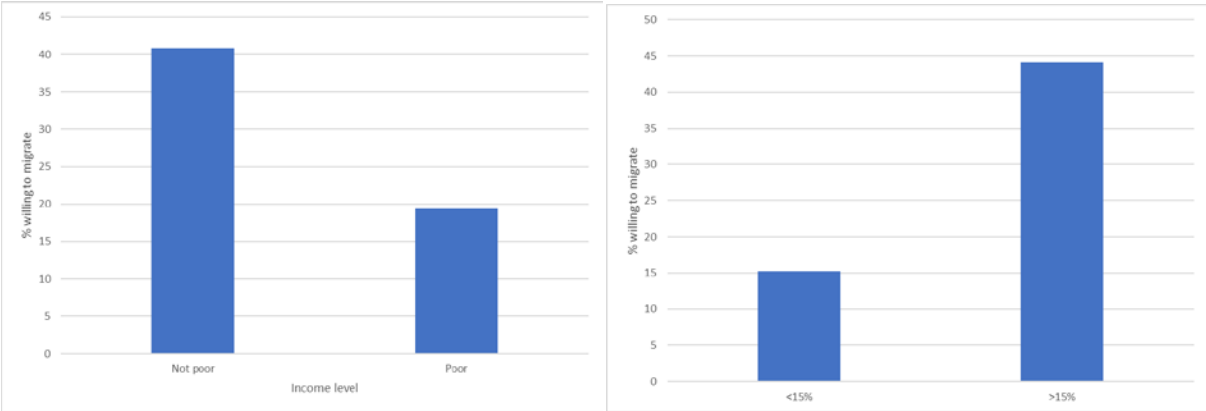

Figure 2.23 Willingness to migrate and poverty. Right: Willingness to migrate and slope residence

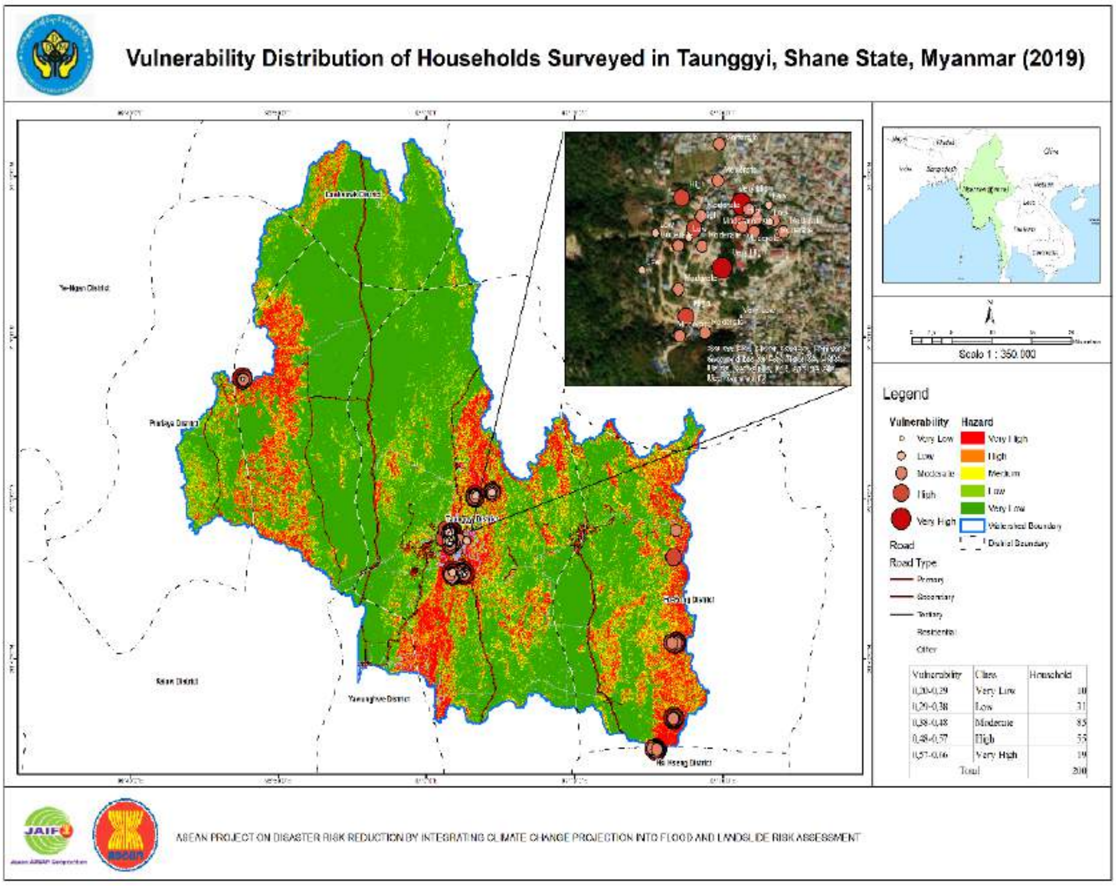

Figure 2.24 Vulnerability distribution of households surveyed in Taunggyi, Shane State, Myanmar (2019)

The spatial distribution of surveyed households with a different level of vulnerability can be referred to the **Figure 2.24** above.

3. Household landslide risk profiles

3.1. Landslide risk profile developed using RCP 4.5 future climate scenarios

This landslide hazard and risk assessment was done based on the concept introduced by the UNDRR (formerly known as UNISDR) as described in the *ASEAN Project for Disaster Risk Reduction by Integrating Future Climate Scenarios into Landslide Risk Assessment* guidelines. A risk assessment was conducted for two different scenarios of RCP 4.5 and RCP 8.5 for three different projected years – 2030, 2050 and 2080.

The results of the risk assessment were presented in five different classes of risk: very high, high, moderate, low and very low. Results show a trend of the moderate, high and very high classes increasing throughout the projected years.

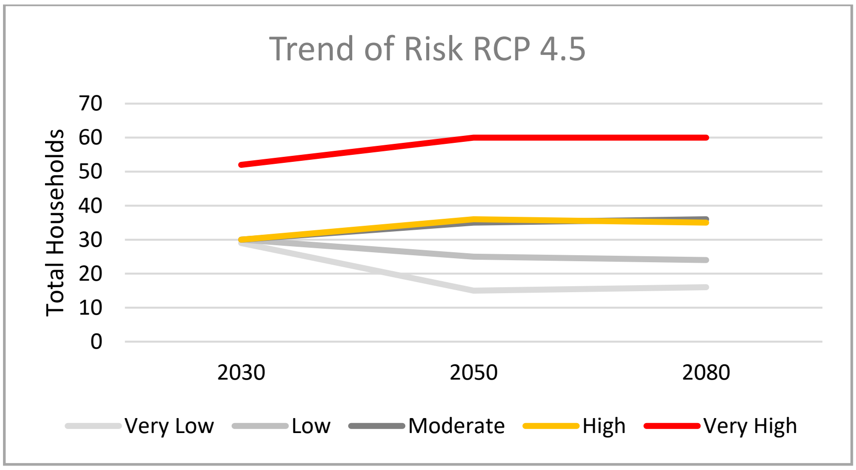

Figure 3.1 Risk trends in Taunggyi RBP (RCP 4.5)

The number of surveyed households that fall under the five categories of risk at the different projected time period of the 2030s, 2050s and 2080s can be seen in **Table 3.1**. It should be noted that the exposure data used in this case study was based on sample data of the surveyed households only. For future studies, it is recommended that projected population and more comprehensive household data be used.

Table 3.1 Distribution of landslide risk of surveyed households for the 2030s, 2050s, and 2080s for RCP 4.5 in Taunggyi RBP

Risk	2030s	2050s	2080s
Very low	29	15	16
Low	30	25	24
Moderate	30	35	36
High	30	36	35
Very high	52	60	60
Grand Total	171	171	171

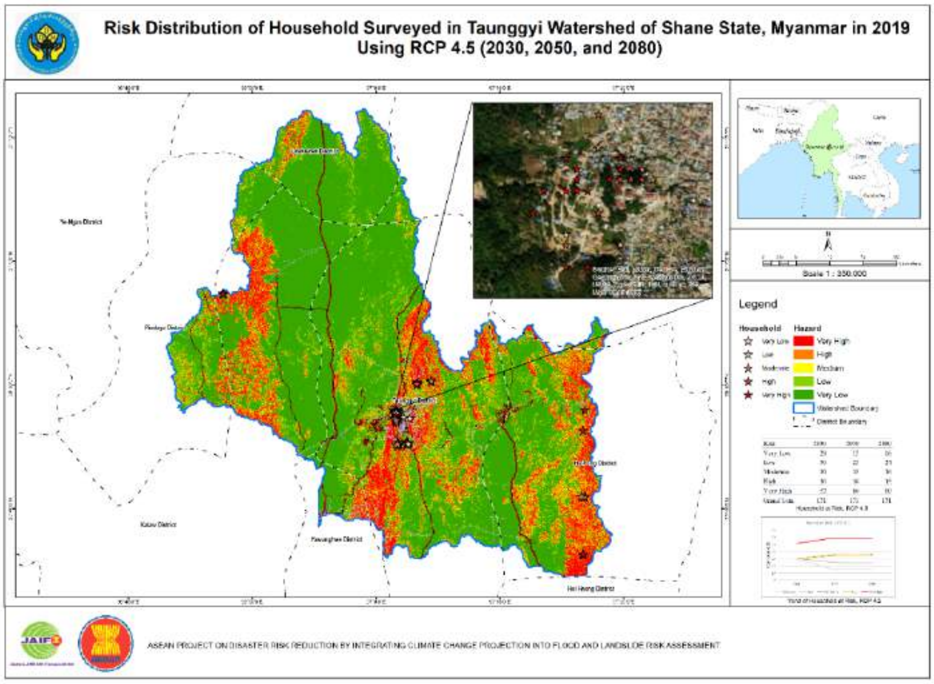

Figure 3.2 Risk distribution of households surveyed in the Taunggyi Watershed of Shane State, Myanmar in 2019 using RCP 4.5 (2030, 2050, and 2080)

The effects of slope angles on landslides

Some studies state that landslides are more common in areas with a less than 15 degree slope. It should be noted however, that more detailed studies are needed in regards to the effect of slope angle on landslides. For this case study, an attempt was made by overlaying the slope angles and landslide risk of surveyed households. This result will provide preliminary information on how many and which high-risk households are located in areas beneath a 15 degree slope angle. This information will be useful as a starting point when developing landslide disaster risk reduction and mitigation strategies.

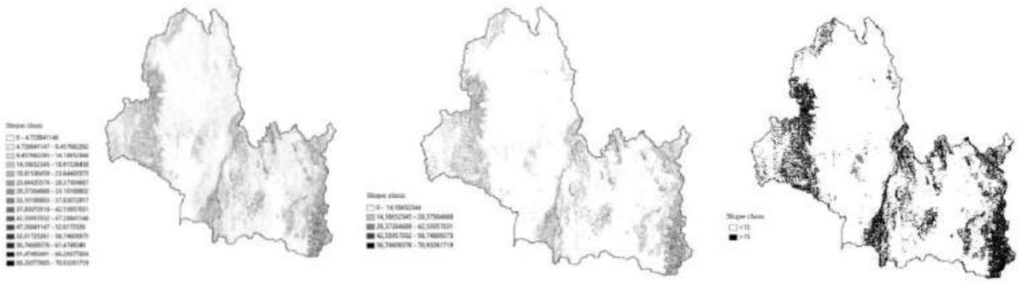

Figure 3.3 Slope classification process

Table 3.2 depicts the cross tabulation between risk and slope for RCP 4.5. The original slope is segmented into 15 classes using the equal interval of Geographic Information Systems to see the distribution of the slope. The classes are then reclassified into 5 classes to determine the majority of the slope classes. The classes range from 0-15, 15-30, 30-45, 45-60, and 60-75. The class is then aggregated into two major classes of <15 and >15 degrees.

Table 3.2 Cross tabulation between risk and slope (RCP 4.5)

Slope Class	Risk Scenario RCP 4.5, Year 2030					Total number of households
	Very low	Low	Moderate	High	Very high	
<15%	13	3	5	4	13	38
>15%	16	27	25	26	39	133
Total	29	30	30	30	52	171
Slope Class	Risk Scenario RCP 4.5, Year 2050					Total Household
	Very Low	Low	Moderate	High	Very High	
<15%	13	3	5	4	13	38
>15%	16	27	25	26	39	133
Total	29	30	30	30	52	171
Slope Class	Risk Scenario RCP 4.5, Year 2080					Total Household
	Very Low	Low	Moderate	High	Very High	
<15%	13	3	5	4	13	38
>15%	16	27	25	26	39	133
Total	29	30	30	30	52	171

3.2. Landslide risk profile developed using future climate scenarios of RCP 8.5

The risk assessment using RCP 8.5 also shows similar results to the assessment using RCP 4.5. The number of surveyed households that fall under high risk and very high risk classes increase throughout the projected years of the 2030s, 2050s and 2080s as shown **in Figure 3.5**. The number of surveyed households that fall under five risk categories at different projected time periods (2030s, 2050s and 2080s) can be seen in **Table 3.3**.

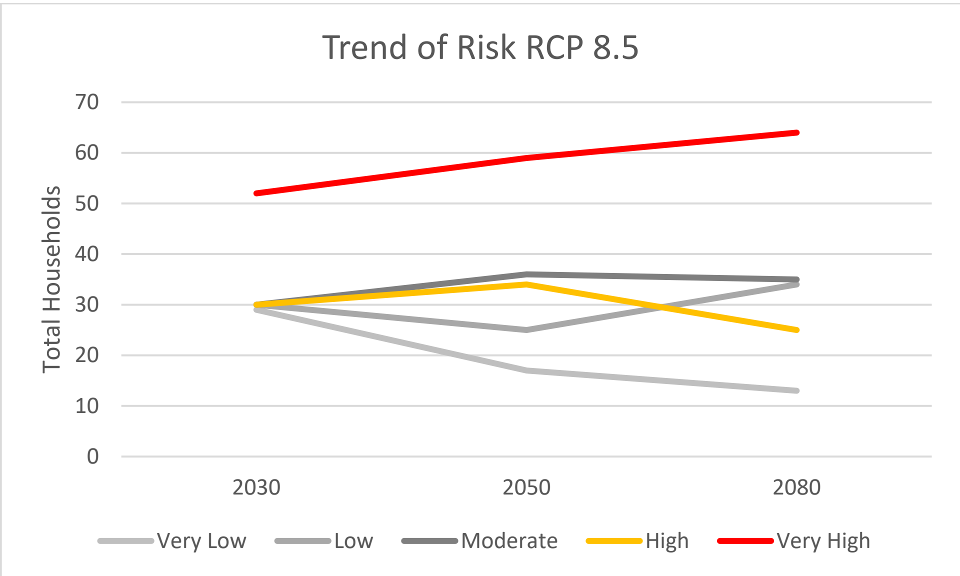

Figure 3.4 Risk trends in Taunggyi RBP (RCP 8.5)

Table 3.3 Distribution of landslide risk of surveyed households for the time periods of the 2030s, 2050s, and 2080s for RCP 8.5 in Taunggyi RBP

Risk	2030s	2050s	2080s
Very low	29	17	13
Low	30	25	34
Moderate	30	36	35
High	30	34	25
Very high	52	59	64
Grand Total	171	171	171

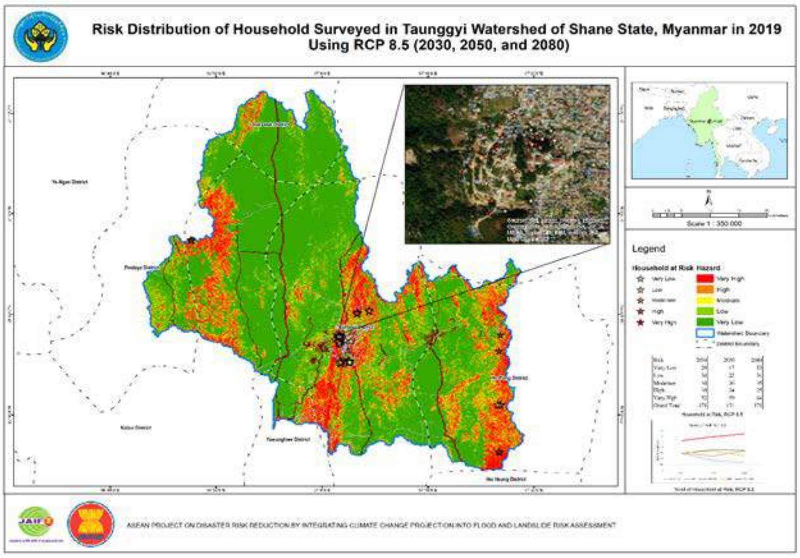

Figure 3.5 Spatial distribution of risk for surveyed households (2019) located at Taunggyi RBP using RCP 8.5 for 2030, 2050, and 2080

Slope angle effect on landslides

A cross-tabulation was also done by overlaying surveyed households with slope angle in the RCP 8.5 climate scenario. Results are shown in **Table 3.4**.

Table 3.4 Cross-tabulation between risk and slope (RCP 8.5)

Slope class	Risk Scenario RCP 8.5, Year 2030					Total households
	Very low	Low	Moderate	High	Very high	
<15%	13	3	5	4	13	38
>15%	16	27	25	26	39	133
Total	29	30	30	30	52	171
Slope class	Risk Scenario RCP 8.5, Year 2050					Total households
	Very low	Low	Moderate	High	Very high	
<15%	13	3	5	4	13	38
>15%	16	27	25	26	39	133
Total	29	30	30	30	52	171
Slope class	Risk Scenario RCP 8.5, Year 2080					Total households
	Very low	Low	Moderate	High	Very high	
<15%	13	3	5	4	13	38
>15%	16	27	25	26	39	133
Total	29	30	30	30	52	171

3.3. Potential Applications

This case study showcases the potential application of developing a landslide risk assessment by integrating future climate change scenarios. The results can be used as a reference to design landslide risk reduction and management strategies and programs, and prioritize the high and very high-risk areas and households that have been identified through the case study. **Table 3.5** shows samples of the suggested action level based on the identified risk condition.

Table 3.5 Suggested risk level and DRR related action level

Risk level	Color code	Action level
Very high	**Red**	**Urgent action -** Very high risk conditions with highest priority for risk reduction & contingency planning.
High	**Orange**	**Immediate action -** High risk conditions with high priority for risk reduction & contingency planning.
Moderate	**Yellow**	**Prompt action –** Moderate to high risk conditions with risk addressed by reduction & contingency planning.
Low	**Light Green**	**Planned action** – Risk conditions sufficiently high to give consideration to further reduction & contingency planning.
Very low	**Green**	**Advisory in nature –** Low risk conditions with additional reduction and contingency planning.

Surveyed household data can also provide important information on vulnerability and capacity, especially for households located in high and very high areas prone to landslides. These details and systematic data can help decision makers to design appropriate DRR strategies. Using GIS technology, where open-source options such as QGIS and Google Earth are also available, surveyed households can be presented as part of an easy and user-friendly tool to help in the decision-making process. **Figure 3.6** shows a sample of households located in high landslide prone areas with detailed information and attributes collected and mapped in Google Earth, where the level of landslide hazard, vulnerability, capacity and risk can be seen.

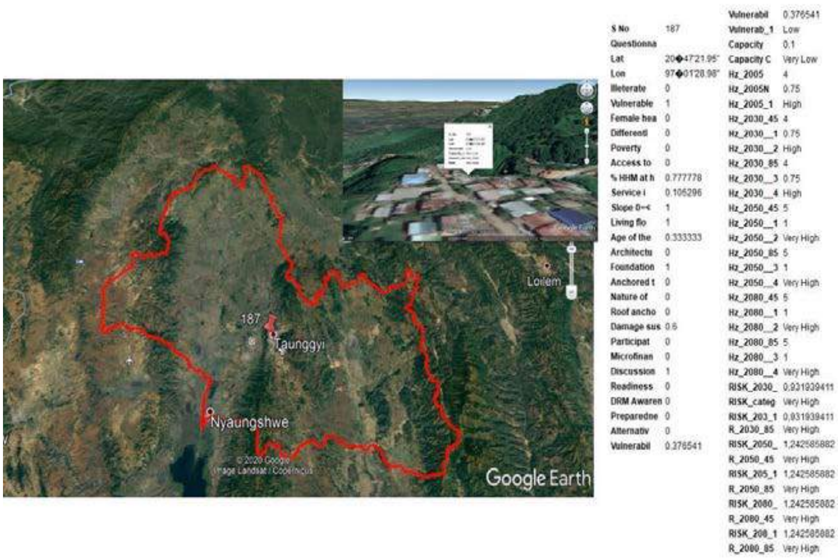

Figure 3.6 Google Earth screenshot showing household samples and attributes

4. Recommendations

Landslide-prone areas in the Taunggyi River Basin have been identified through this case study. This study can be replicated in other river basins in Myanmar in order to get a comprehensive picture of landslide risk in the country that in the end can be used to identify programming gaps and opportunities that will enable government and other relevant agencies to formulate landslide risk reduction plans and strategies. The landslide hazard maps and surveyed household and statistical data that were generated as a result of this study can be used as a model (to be adapted and replicated in other river basins, especially for those prone to landslides) and be integrated into the local and national disaster risk management framework in Myanmar in the following ways.

- The hazard maps can be used by policy makers, decision makers and planners as a basis for future master plans and safe development. Authorities can take necessary actions to reduce the potential impacts of landslides on various economic sectors such as transport, housing, etc.
- The hazard maps and statistical data can help policy makers, decision makers, planners and other parties to plan and implement effective landslide risk management strategies in Myanmar, particularly at the river basin scale.
- Prevention and response related agencies can use the hazard maps to coordinate prevention and response strategies and identify sites for structural and non-structural mitigation programs and initiatives.
- The hazard maps could help local government in introducing and enforcing building codes and permitting regulations to protect homes and infrastructure.
- The case study report – the hazard, vulnerability and risk maps – can be used as a tool to educate and create public awareness on landslide hazard and risk.
- Development of community-based landslide risk reduction and management can be initiated, especially for those communities prone to landslide in the high and very high categories.

The landslide hazard and risk assessment in this case study was carried out using scientific tools and relevant methods and outputs were generated on the appropriate scale. For the extensive hazard assessment and mapping, several datasets were required: geological, hydro-meteorological, geo-morphological and other related data. Though some information was available, a large quantity of data was missing. It is recommended, when better resources such as better resolution datasets become available in future, that more detailed analyses and landslide research are conducted in the high and very high susceptible zones.

5. REFERENCES

Related to Landslide:

Aditian, A., Kubota T., Shinohara, Y., Comparison of GIS-based landslide susceptibility models using frequency ratio, logistic regression, and artificial neural network in a tertiary region of Ambon, Indonesia, Geomorphology, Volume 318, 2018, Pages 101-111.

Barbieri, G., & Cambuli, P. (2009). The weight of evidence statistical method in landslide susceptibility mapping of the Rio Pardu Valley (Sardinia, Italy) (Vol. 18, pp. 2658–2664). Presented at the Proceedings of.

Baum, R. L., Savage, W. Z., & Godt, J. W. (2009). *TRIGRS-A Fortran Program for Transient Rainfall Infiltration and Grid-Based Regional Slope- Stability Analysis, Version 2.0*. United States Geological Survey.

Che, V. B., Kervyn, M., Ernst, G., Trefois, P., Ayonghe, S., Jacobs, P., … Suh, C. E. (2011). Systematic documentation of landslide events in Limbe area (Mt Cameroon Volcano, SW Cameroon): geometry, controlling, and triggering factors. *Natural Hazards*, *59*(1), 47–74.

Dai, F.C., Lee, C.F., 2002. Landslide characteristics and slope instability modelling using GIS, Lantau Island, Hong Kong. Geomorphology 42:213–228. https://doi.org/10.1016/ S0169-555X(01) 00087-3.

Georisk-Project. (2015). Technical manual: Landslides susceptibility analysis with bivariate statistic using ArcGIS 10.x (Panduan teknis: analisa gerakan tanah dengan metode statistik bivariate menggunakan ArcGIS 10.x. German-Indonesian Technical Cooperation on Mitigation of Georisk.

Lee, S., Pradhan, B. Probabilistic landslide hazards and risk mapping on Penang Island, Malaysia. J Earth Syst Sci 115, 661–672 (2006). https://doi.org/10.1007/s12040-006-0004-0

Lee, S., Pradhan, B., 2007. Landslide hazard mapping at Selangor, Malaysia using frequency neural network model at Cameron Highland, Malaysia. Landslides 7, 13–30.

Sumaryono, Muslim, D., Sulaksana, N., & Triana, Y. D. (2015). Weights of evidence method for landslide susceptibility mapping in Tandikek and Damar Bancah, West Sumatra, Indonesia. *International Journal of Science and Research*, *4*(10).

van Westen, C. J. (2002). Use of weights of evidence modeling for landslide susceptibility mapping. International Institute for Geoinformation Science and Earth Observation (ITC).

Van Westen, C., Van Asch, T. W., & Soeters, R. (2006). Landslide hazard and risk zonation—why is it still so difficult? *Bulletin of Engineering Geology and the Environment*, *65*(2), 167–184.

Related to Climate Change:

Hernaman V, Grose M and Clarke JM (2017) Evaluating the performance of the latest climate models over Southeast Asia. CSIRO, Australia; Report for ADB, 2017

The Intergovernmental Panel on Climate Change (IPCC)'s Task Group on Data and Scenario Support for Impact and Climate Assessment (TGICA) also provides general guidelines on the use of data and scenario in impact and adaptation assessments. http://www.ipcc-data.org/guidelines/#ClimScenSD

Katzfey, JJ, McGregor, JL and Suppiah, R (2014). High-Resolution Climate Projections for Vietnam: Technical Report. CSIRO, Australia. 266 pp.

Wilby, R.L. et al. 1998. Statistical downscaling of general circulation model output: a comparison of methods. Water Resources Research 34(11): 2995–3008.

Ahmadalipour A, Rana A, Moradkhani H and Sharma A. 2015 Multi-Criteria evaluation of CMIP5 GCMs for Climate Change Impact Analysis. Theoretical and Applied Climatology.

Arora, M., Goel, N. K. & Singh, P. (2005). Evaluation of temperature trends over India. Hydrol. Sci. J., 50(1), 81–93. doi:10.1623/hysj.50.1.81.56330

Asokan SM, Rogberg P, Bring A, Jarsjo J and Destouni G 2016. Climate model performance and change projection for freshwater fluxes: Comparison for irrigated areas in Central and South Asia, Journal of Hydrology: Regional Studies 5: 48–65. DOI: 10.1016/j.ejrh.2015.11.017

Barbero, R., Fowler, H. J., Lenderink, G., & Blenkinsop, S. (2017). Is the intensification of precipitation extremes with global warming better detected at hourly than daily resolutions? Geophysical Research Letters, 44, 974– 983. https://doi.org/10.1002/2016GL071917

2, C.M. et al. (2009) 'Bayesian multi-model projection of climate: Bias assumptions and interannual variability', Climate Dynamics, Vol. 33, No. 6, pp.849–868.

Carter, T.R., R.N. Jones, X. Lu, S. Bhadwal, C. Conde, L.O. Mearns, B.C. O'Neill, M.D.A. Rounsevell, and M.B. Zurek, 2007: New assessment methods and the characterisation of future conditions. In: Climate Change 2007. Impacts, Adaptation and Vulnerability. Contribution of Working Group II to the Fourth Assessment Report of the Intergovernmental Panel on Climate Change [Parry, M.L., O.F. Canziani, J.P. Palutikof, P.J. Van Der Linde, and C.E. Hanson (eds.)]. Cambridge University Press, Cambridge, UK, pp. 133-171.

Christensen, J.H., B. Hewitson, A. Busuioc, A. Chen, X. Gau, I. Held, R. Jones, R. Kolli, W. Kwon, R. Laprise, V. Magaña Rueda, L. Mearns, C. Menéndez, J. Räisänen, A. Rinke, A. Sarr, and P. Whetton, 2007: Regional climate projections. In: Climate Change 2007: The Physical Science Basis. Contribution of Working Group I to the Fourth Assessment Report of the Intergovernmental Panel on Climate Change [Solomon, S., D. Qin, M. Manning, Z. Chen, M. Marquis, K.B. Averyt, M. Tignor and H.L. Miller (eds.)]. Cambridge University Press, Cambridge, UK, pp. 847-940.

Collins, M., R. Knutti, J. Arblaster, J.-L. Dufresne, T. Fichefet, P. Friedlingstein, et al. 2013 Long-term climate change: projections, commitments and irreversibility T.F. Stocker, D. Qin, G.-K. Plattner, M. Tignor, S.K. Allen, J. Boschung, et al. (Eds.), Climate Change 2013: The Physical Science Basis. Contribution of Working Group I to the Fifth Assessment Report of the Intergovernmental Panel on Climate Change, Cambridge University Press Cambridge, United Kingdom and New York, NY, USA.

Cruz RV, Harasawa H, Lal M, Wu S, Anokhin Y, Punsalmaa B, Honda Y, Jafari M, Li C, Huu N (2007) Asia. Climate change, 2007, impacts, adaptation and vulnerability. In: Parry ML, Canziani OF, Palutikof JP et al (eds) Contribution of Working Group II to the Fourth Assessment Report of the Intergovernmental Panel on Climate Change. Cambridge University Press, Cambridge, pp 469–506.

Dangendorf, S. et al. 2017 Reassessment of 20th century global mean sea level rise. Proc. Natl Acad. Sci. 114: 5946–5951.

Dash, S.K., Jenamani, R.K., Kalsi, S.R., & Panda, S.K. (2007). Some evidence of climate change in twentieth-century India. Climatic Change, 85, 299–321. doi:10.1007/s10584-007-9305-9

Demirel, M.C. and Moradkhani, H. 2016 Assessing the impact of CMIP5 climate multi-modeling on estimating the precipitation seasonality and timing, Climatic Change. 135(2); 357–372.

Field, C.B., Barros, V.R., Dokken, D.J., Mach, K.J., Mastrandrea, M.D., Bilir, T.E., Chatterjee, M., Ebi, K.L., Estrada, Y.O., Genova, R.C., Girma, B., Kissel, E.S., Levy, A.N., MacCracken, S., Mastrandrea, P.R., & White, L.L. (Eds.) (2014). What's in it for South Asia? Executive summary from IPCC, 2014. Climate Change 2014: Impacts, Adaptation, and Vulnerability. Contribution of Working Group II to the Fifth Assessment Report of the Intergovernmental Panel on Climate Change. Cambridge, United Kingdom & New York USA: Cambridge University Press. http://cdkn.org/wpcontent/uploads/2014/04/CDKN-IPCC-Whats-in-it-for-South-Asia-AR5.pdf

Goswami, B.N., Venugopal, V., Sengupta, D., Madhusoodanam, M.S., &Xavier, P.K. (2006). Increasing trends of extreme rain events over India in a warming environment. Science, 314, 1442–1445.doi: 10.1126/science.1132027

Guha-Sapir D, Hoyois P and Regina B. 2013 Annual Disaster Statistical Review 2012:The Numbers and Trends. Brussels: CRED. http://www.cred.be/sites/default/files/ADSR_2012.pdf [Accessed: 20 October 2019]

Hernaman V, Grose M and Clarke JM 2017. Evaluating the performance of the latest climate models over Southeast Asia. Asian Development Bank, Australia: CSIRO.

Hay CC, Morrow E, Kopp RE and Mitrovica JX. 2015 Probabilistic reanalysis of twentieth-century sea-level rise. Nature. 517: 481–484.

Hijioka, Y., E. Lin, J.J. Pereira, R.T. Corlett, X. Cui, G.E. Insarov, R.D. Lasco, E. Lindgren, and A. Surjan, 2014: Asia.

In: Climate Change 2014: Impacts, Adaptation, and Vulnerability. Part B: Regional Aspects. Contribution of Working Group II to the Fifth Assessment Report of the Intergovernmental Panel on Climate Change [Barros, V.R., C.B. Field, D.J. Dokken, M.D. Mastrandrea, K.J. Mach, T.E. Bilir, M. Chatterjee, K.L. Ebi, Y.O. Estrada, R.C. Genova, B. Girma, E.S. Kissel, A.N. Levy, S. MacCracken, P.R. Mastrandrea, and L.L. White (eds.)]. Cambridge University Press, Cambridge, United Kingdom and New York, NY, USA, pp. 1327-1370.

Hoerling, M., J. Eischeid, J. Perlwitz, X. Quan, T. Zhang, and P. Pegion. 2012. On the Increased Frequency of Mediterranean Drought. Journal of Climate 25:2146–2161. doi: http://dx.doi.org/10.1175/JCLI-D-11-00296.1

IPCC 2014: Climate Change 2014: Synthesis Report. Contribution of Working Groups I, II and III to the Fifth Assessment Report of the Intergovernmental Panel on Climate Change [Core Writing Team, R.K. Pachauri and L.A. Meyer (eds.)]. IPCC, Geneva, Switzerland, 151 pp.

IPCC, 2012: Managing the Risks of Extreme Events and Disasters to Advance Climate Change Adaptation. A Special Report of Working Groups I and II of the Intergovernmental Panel on Climate Change [Field, C.B., V. Barros, T.F. Stocker, D. Qin, D.J. Dokken, K.L. Ebi, M.D. Mastrandrea, K.J. Mach, G.-K. Plattner, S.K. Allen, M. Tignor, and P.M. Midgley (eds.)]. Cambridge University Press, Cambridge, UK, and New York, NY, USA, 582 pp.

IPCC 2007 Climate Change 2007: the physical science basis. In: Solomon S, Quin D, Manning M, Chen X, Marquis M, Averyt KB, Tignor HL, Miller M (eds) Contribution of Working Group I to the Fourth Assessment Report of the Intergovernmental Panel on Climate Change. Cambridge University Press, Cambridge, pp 1–996.

Katzfey, JJ, McGregor, JL and Suppiah, R (2014). High-Resolution Climate Projections for Vietnam: Technical Report. CSIRO, Australia. 266 pp.

Khan, T.M.A., Singh, O.P., & Sazedur Rahman, M.D. (2000). Recent sea level and sea surface temperature trends along the Bangladesh coast in relation to the frequency of intense cyclones. Marine Geodesy, 23, 103–116. doi:10.1080/01490410050030670

Krishnamurthy, K. & Shukla, J. (2000). Intraseasonal and Interannual Variability of Rainfall over India.
Journal of Climate, 13, 466-4377. doi:10.1175/1520-0442(2000)013<0001:IAIVOR>2.0.CO;2

Krishnamurthy, C.K.B., Lall, U., & Kwo, H. (2009). Changing Frequency and intensity of rainfall extremes over India from 1951 to 2003. Journal of Climate, 22, 4737-4746. doi: 10.1175/2009JCLI2896.1

Knutti, R., G. Abramowitz, M. Collins, V. Eyring, P.J. Glecker, B. Hewitson, and L. Mearns, 2010b: Good practice guidance paper on assessing and combining multi model climate projections. In: Meeting Report of the Intergovernmental Panel on Climate Change Expert Meeting on Assessing and Combining MultiModel Climate Projections [Stocker, T.F., Q. Dahe, G.-K. Plattner, M. Tignor, and P.M. Midgley (eds.)]. IPCC Working Group I Technical Support Unit, University of Bern, Bern, Switzerland, pp. 1-13.

Kulp SA and Strauss BH. 2019 New elevation data triple estimates of global vulnerability to sea-level rise and coastal flooding. Nature Communications 10:4844 https://doi.org/10.1038/s41467-019-12808-z.

Lacombe, G., & McCartney, M. (2014). Uncovering consistencies in Indian rainfall trends observed over the last half century. Climatic Change. 123: 287–299. doi: 10.1007/s10584-013-1036-5

Lal, M. (2003). Global climate change: India’s monsoon and its variability. Journal of Environmental Studies & Policy, 6, 1–34.

Lenderink, G., and E. van Meijgaard. 2010. Linking Increases in Hourly Precipitation Extremes to Atmospheric Temperature and Moisture Changes. Environment Research Letters 5(2). http://iopscience.iop.org/1748-9326/5/2/025208/.

Meinshausen MSJ, Smith K, Calvin JS, Daniel MLT, Kainuma and et al.: 2011 The RCP greenhouse gas concentrations and their extensions from 1765 to 2300. Climatic Change. 109: 213-241.

Meher JK, Das L, Akhter J, Benestad RE and Mezghani A. 2017. Performance of CMIP3 and CMIP5 GCMs to Simulate Observed Rainfall Characteristics over the Western Himalayan Region, Journal of Climate 30(19):7777-7799. DOI: 10.1175/JCLI-D-16-0774.1

Min, S.-K., X. Zhang, F. Zwiers, and G. Hegerl. 2011. Human Contribution to More Intense Precipitation Extremes. Nature. 470:378–381 http://www.nature.com/nature/journal/v470/n7334/full/nature09763.html.

Min, S.K., Kwon, W.T., Park, E.H., & Choi, Y. (2003). Spatial and temporal comparisons of droughts over Korea with East Asia. International Journal of Climatology, 23, 223–233. doi:10.1002/joc.872

Mirza, M.Q. (2002). Global warming and changes in the probability of occurrence of floods in Bangladesh and implications. Global Environmental Change, 12, 127–138. doi:10.1016/S0959-3780(02)00002-X

O'Gorman, P. A., and T. Schneider. 2009. The Physical Basis for Increases in Precipitation Extremes in Simulations of 21st-century Climate Change. Proceedings of the National Academy of Sciences 106(35): 14773–14777.

http://www.pnas.org/content/106/35/14773.short

Mora, C., B. Dousset, I.R. Caldwell, F.E. Powell, R.C. Geronimo, R. Bielecki Coral, et al. Global risk of deadly heat. Nat. Clim. Chang., 7: 501-506.

Pant, G. B., & Kumar, K. R. (1997). Climates of South Asia. Chichester: John Wiley & Sons Ltd.

Pepin, Nicholas & Bradley, Raymond & Diaz, Henry & Baraer, Michel & Cáceres, Bolívar & Forsythe, Nathan & Fowler, Hayley & Greenwood, Gregory & Hashmi, Muhammad & Liu, X. & Miller, J. & Ning, Liang & Ohmura, Atsumu & Palazzi, Elisa & Rangwala, Imtiaz & Schöner, Wolfgang & Severskiy, I. & Shahgedanova, M. & Wang, M. & Yang, Daqing. (2015). Elevation-dependent warming in mountain regions of the world. Nature Climate Change. 5. 424-430. 10.1038/nclimate2563.

Prasanna V 2015. Regional climate change scenarios over South Asia in the CMIP5 coupled climate model simulations, Meteorol. Atmos. Phys. 127(5): 561-578. DOI: 10.1007%2Fs00703-015-0379-z

Preethi B, Mujumdar M, Prabhu A and Kripalani R. 2017. Variability and Teleconnections of South and East Asian Summer Monsoons in Present and Future Projections of CMIP5 Climate Models, Asia-Pacific Journal of Atmospheric Sciences 53(2): 305-325. DOI: 10.1007/s13143-017-0034-3

Qalbi HB, Faqih A and Hidayat R. 2017. Future rainfall variability in Indonesia under different ENSO and IOD composites based on decadal predictions of CMIP5 datasets. IOP Conf. Series: Earth and Environmental Science 54 (2017) 012043. doi:10.1088/1755-1315/54/1/012043

Rahmstorf, S., and D. Coumou. 2011. Increase of Extreme Events in a Warming World. Proceedings of National Academy of Sciences of the United States of America. 108(44): 17905–17909.

Randall, D.A., R.A. Wood, S. Bony, R. Colman, T. Fichefet, J. Fyfe, V. Kattsov, A. Pitman, J. Shukla, J. Srinivasan, R.J. Stouffer, A. Sumi, and K.E. Taylor, 2007: Climate models and their evaluation. In: Climate Change 2007: The Physical Science Basis. Contribution of Working Group I to the Fourth Assessment Report of the Intergovernmental Panel on Climate Change [Solomon, S., D. Qin, M. Manning, Z. Chen, M. Marquis, K.B. Averyt, M. Tignor and H.L. Miller (eds.)]. Cambridge University Press, Cambridge, UK, and New York, NY, pp. 589-662.

Rupp, D.E. et al. (2013) 'Evaluation of CMIP5 20th century climate simulations for the Pacific Northwest US', Journal of Geophysical Research Atmospheres, April, Vol. 118, No. 19, pp.10884-10906 [online] https://doi.org/10.1002/jgrd.50843.

Roy SS and Balling SC 2004. Trends in extreme daily precipitation indices in India. Internal Journal of Climatology. 24(4): 457-466. doi: https://doi.org/10.1002/joc.995.

Roxy M.K., Ghosh S., Pathak, A., Athulya R., Mujumdar M., Murtugudde R., Terray P. and Rajeevan M. (2017). "A threefold rise in widespread extreme rain events over central India". Nature Communications. 8 (1): 708. doi:10.1038/s41467-017-00744-9

Seneviratne, S.I., N. Nicholls, D. Easterling, C.M. Goodess, S. Kanae, J. Kossin, Y. Luo, J. Marengo, K. McInnes, M. Rahimi, M. Reichstein, A. Sorteberg, C. Vera, and X. Zhang, 2012: Changes in climate extremes and their impacts on the natural physical environment. In: Managing the Risks of Extreme Events and Disasters to Advance Climate Change Adaptation [Field, C.B., V. Barros, T.F. Stocker, D. Qin, D.J. Dokken, K.L. Ebi, M.D. Mastrandrea, K.J. Mach, G.-K. Plattner, S.K. Allen, M. Tignor, and P.M. Midgley (eds.)]. A Special Report of Working Groups I and II of the Intergovernmental Panel on Climate Change (IPCC). Cambridge University Press, Cambridge, UK, and New York, NY, USA, pp. 109-230.

Singh C, Ganguly D and Dash SK 2017. On the dust load and rainfall relationship in South Asia: an analysis from CMIP5, Climate Dynamics. 50(1-2): 403-422. DOI 10.1007/s00382-017-3617-x

Sivakumar MVK and Stefanski R 2015 Climate Change in South Asia. R. Lal et al. (eds.), Climate Change and Food Security in South Asia, 13. Doi: 10.1007/978-90-481-9516-9_2.

Sharma, A., Wasko, C., & Lettenmaier, D.P. (2018). If precipitation extremes are increasing, why aren't Woods?. Water Resources Research, 54, 8545–8551.
https://doi.org/10.1029/2018WR023749

Shrestha, A.B., Wake, C.P., Dibb, J.E., & Mayewski, P.A. (2000). Precipitation fluctuations in the Nepal Himalaya and its vicinity and relationship with some large-scale climatological parameters. International Journal of Climatology, 20, 317–327. doi:10.1002/(SICI)1097-0088(20000315)20:3<317: AID-JOC476>3.0.CO;2-G

Singapore Red Cross. 2010. https://reliefweb.int/report/pakistan/pakistan-floodsthe-deluge-disaster-facts-figures-15-september-2010 [Accessed 20 November 2019]

Sperber, K.R., Annamalai, H., Kang, I.S., Kitoh, A., Moise, A., Turner, A., Wang, B., & Zhou, T. (2013). The Asian summer monsoon: an intercomparison of CMIP5 vs. CMIP3 simulations of the late 20th century. Climate Dynamics, 41, 2711-2744. doi:10.1007/s00382-012-1607-6

Stott, P., D. Stone, and M. Allen. 2004. Human Contribution to the European Heatwave of 2003. Nature. 432:610–614.
http://www.nature.com/nature/journal/v432/n7017/abs/nature03089.html

Trenberth, K. E. 2005. The Impact of Climate Change and Variability on Heavy Precipitation, Floods, and Droughts. In M. G. Anderson, ed. Encyclopedia of Hydrological Sciences. John Wiley & Sons, Ltd. http://acacia.ucar.edu/cas/Trenberth/EHShsa211.pdf.

Taylor KE, Ronald JS and Gerald AM 2012 An Overview of CMIP5 and the Experiment Design. Bull. Amer. Meteor. Soc. 93: 485–498.

Annex 1. Surveyed household database (2019)

				Sensitivity																	Capacity						
				Socio-economic								Physical															
S No	Questionnaire No	Lat	Lon	Illeterate household	Vulnerable population	Female headed HH	Differently abled	Poverty	Access to Health Center	% HHM at home	Service interruption	Slope 0=<15% 1=>15%	Living floor	Age of the building	Architectural Approval	Foundation type	Anchored to bedrock	Nature of walls	Roof anchorage	Damage suscept. Rating	Participation in DRMP	Microfinance	Discussion on LS before rainy	Readiness to migrate	DRM Awareness	Preparedness	Alternative road
			Weightage=>				30%									70%					20	10	10	5	10	35	10
1		20'47'33.3"	97'01'37.8"	0	1	1	0	0	0	0,61	0,11	1	1	0,00	0	1	1	0	0	0,70	1	1	1	1	1	0	1
2		20'47'33"	97'01'37.3"	0	1	1	0	0	0	0,64	0,07	1	0	0,33	0	0	1	0	0	0,70	1	0	1	1	1	1	1
3		20'47'32.9"	97'01'38.3"	0	1	0	0	0	0	0,73	0,15	1	0	0,44	0	0	1	0	0	0,80	0	0	1	1	1	0	1
4		20'47'32.5"	97'01'37.4"	0	1	1	0	0	0	0,81	0,12	1	1	0,33	1	1	1	0	0	0,90	1	0	0	0	1	0	1
5		20'47'30.6"	97'01'37.3"	0	1	0	1	0	0	0,59	0,18	1	1	0,33	0	1	1	1	0	0,30	0	0	0	1	1	0	0
6		20'47'30.0"	97'01'40.9"	0	1	0	0	0	0	1,00	0,29	1	0	0,22	0	1	1	1	0	0,40	0	0	0	1	1	0	0
7		20'47'28.2"	97'01'39.9"	0	1	0	0	0	0	0,83	0,14	1	0	0,33	0	1	1	0	1	0,50	0	0	0	1	1	0	0
8		20'47'22.7"	97'01'38.8"	0	1	1	0	0	0	0,76	0,14	1	0	0,33	0	1	1	1	1	0,50	0	0	0	0	1	0	0
9		20'47'22.7"	97'01'42.8"	0	1	0	0	0	0	0,78	0,16	0	1	0,00	0	1	1	0	0	0,30	0	0	0	0	1	0	0
10		20'47'31.0"	97'01'38.3"	0	1	1	0	0	0	1,00	0,10	1	1	0,22	1	1	1	0	0	0,40	0	0	1	1	1	0	0
11		20'47'26.9"	97'02'11.16"	0	1	0	0	0	0	0,86	0,17	0	1	0,33	1	1	1	0	0	0,10	0	0	1	0	1	0	1
12		20'47'13.06"	97'01'50.26"	0	1	1	0	0	0	0,83	0,09	0	1	0,56	1	1	1	0	0	0,40	0	0	1	0	1	0	1
13		20'47'13.29"	97'01'50.34"	0	1	0	0	0	0	0,97	0,08	0	1	0,22	0	1	1	1	0	0,30	0	0	1	0	1	0	0
14		20'47'22.77"	97'01'37.53"	0	1	0	0	0	0	0,50	0,08	1	1	0,00	1	1	1	1	0	0,20	0	0	1	1	1	1	0
15		20'47'31.3"	97'01'38.5"	0	1	0	0	0	0	0,89	0,38	1	0	0,00	0	0	1	0	0	0,40	0	0	0	1	1	0	1
16		20'47'31.7"	97'01'38.8"	0	1	1	0	0	0	0,81	0,39	1	0	0,33	0	0	1	0	0	0,40	0	0	0	1	1	0	1
17		20'47'24.3"	97'01'38.7"	0	1	1	0	0	0	0,72	0,17	1	0	0,33	0	0	1	0	0	0,90	0	0	0	0	1	0	1
18		20'47'24.7"	97'01'39.3"	0	1	0	0	0	0	0,63	0,22	0	0	0,22	0	0	1	0	0	0,70	0	0	0	1	1	0	1
19		20'47'24.8"	97'01'38.9"	0	1	0	1	0	0	1,00	0,09	1	0	0,22	0	0	1	0	0	0,80	0	1	1	1	1	1	1
20		20'47'29.78"	97'01'39.9"	0	1	0	0	0	0	0,67	0,21	1	0	0,00	0	1	1	0	0	0,80	0	0	1	1	1	1	1
21		20'47'24.6"	97'01'38.7"	0	1	0	0	0	0	0,89	0,20	1	0	0,00	0	1	1	0	0	0,70	1	0	1	1	1	1	1
22		20'47'25"	97'01'38"	0	1	0	0	0	0	0,80	0,17	1	0	0,22	0	0	1	0	0	0,90	1	0	1	1	1	0	1
23		20•47'34"	96'1' 42"	0	1	0	0	0	0	0,92	0,19	0	1	0,00	1	0	1	0	0	0,50	1	1	0	0	1	0	0
24		20' 47' 50.63"	097' 01' 46.45"	0	1	0	0	0	0	1,00	0,14	1	1	0,00	1	1	1	1	0	0,70	1	1	1	0	1	0	1
25		20' 47' 23.99"	097' 01' 39.48"	0	1	0	0	0	0	0,89	0,18	1	1	0,33	1	0	1	1	0	0,60	1	0	1	0	1	1	0

Vulnerability	Vulnerability Class	Capacity	Capacity Class	Hazard Scenario														RISK											
																		2030_45		2030_85		2050_45		2050_85		2080_45		2080_85	
				2005	2005N	2030_4!	2030_4!	2030_8!	2030_8!	2050_4!	2050_4!	2050_8!	2050_8!	2080_4!	2080_4!	2080_8!	2080_85	RISK	RISK_categor	RISK	R_2030_	RISK	R_2050_	RISK	R_2050_	RISK	R_2080_	RISK	R_2080_
0,47	Moderate	0,65	High	3	0,50	3	0,50	3	0,50	4	0,75	4	0,75	4	0,75	5	1,00	0,11867	Very Low	0,11867	Very Low	0,178	Low	0,178	Low	0,178	Low	0,23733	Low
0,34	Low	0,90	Very High	3	0,50	3	0,50	3	0,50	4	0,75	4	0,75	4	0,75	5	1,00	0,06188	Very Low	0,06188	Very Low	0,09282	Very Low	0,09282	Very Low	0,09282	Very Low	0,12377	Very Low
0,32	Low	0,35	Low	2	0,25	3	0,50	3	0,50	4	0,75	4	0,75	4	0,75	4	0,75	0,15222	Low	0,15222	Low	0,22833	Low	0,22833	Low	0,22833	Low	0,22833	Low
0,59	Very High	0,40	Moderate	1	0,00	2	0,25	2	0,25	2	0,25	2	0,25	2	0,25	3	0,50	0,12269	Very Low	0,12269	Very Low	0,12269	Very Low	0,12269	Very Low	0,12269	Very Low	0,24538	Low
0,54	High	0,15	Very Low	4	0,75	4	0,75	4	0,75	5	1,00	5	1,00	5	1,00	5	1,00	0,89467	Very High	0,89467	Very High	1,19289	Very High	1,19289	Very High	1,19289	Very High	1,19289	Very High
0,45	Moderate	0,15	Very Low	3	0,50	4	0,75	4	0,75	5	1,00	4	0,75	5	1,00	5	1,00	0,73472	High	0,73472	High	0,97963	Very High	0,73472	High	0,97963	Very High	0,97963	Very High
0,45	Moderate	0,15	Very Low	2	0,25	2	0,25	2	0,25	3	0,50	3	0,50	3	0,50	3	0,50	0,24737	Low	0,24737	Low	0,49474	High	0,49474	High	0,49474	High	0,49474	High
0,56	High	0,10	Very Low	4	0,75	4	0,75	4	0,75	5	1,00	5	1,00	5	1,00	5	1,00	1,39232	Very High	1,39232	Very High	1,85643	Very High	1,85643	Very High	1,85643	Very High	1,85643	Very High
0,33	Low	0,10	Very Low	1	0,00	1	0,00	1	0,00	2	0,25	2	0,25	2	0,25	2	0,25	0	Very Low	0	Very Low	0,27156	Moderate	0,27156	Moderate	0,27156	Moderate	0,27156	Moderate
0,55	High	0,25	Low	2	0,25	2	0,25	2	0,25	3	0,50	3	0,50	3	0,50	3	0,50	0,18265	Low	0,18265	Low	0,3653	Moderate	0,3653	Moderate	0,3653	Moderate	0,3653	Moderate
0,42	Moderate	0,30	Low	1	0,00	1	0,00	1	0,00	2	0,25	2	0,25	2	0,25	2	0,25	0	Very Low	0	Very Low	0,11573	Very Low	0,11573	Very Low	0,11573	Very Low	0,11573	Very Low
0,49	High	0,30	Low	4	0,75	5	1,00	5	1,00	5	1,00	5	1,00	5	1,00	5	1,00	0,54448	High	0,54448	High	0,54448	High	0,54448	High	0,54448	High	0,54448	High
0,43	Moderate	0,20	Low	4	0,75	5	1,00	5	1,00	5	1,00	5	1,00	5	1,00	5	1,00	0,70723	High	0,70723	High	0,70723	High	0,70723	High	0,70723	High	0,70723	High
0,54	High	0,60	High	4	0,75	4	0,75	4	0,75	5	1,00	5	1,00	5	1,00	5	1,00	0,22334	Low	0,22334	Low	0,29779	Moderate	0,29779	Moderate	0,29779	Moderate	0,29779	Moderate
0,27	Very Low	0,25	Low	2	0,25	2	0,25	2	0,25	3	0,50	3	0,50	3	0,50	3	0,50	0,0897	Very Low	0,0897	Very Low	0,17941	Low	0,17941	Low	0,17941	Low	0,17941	Low
0,33	Low	0,25	Low	2	0,25	2	0,25	2	0,25	3	0,50	3	0,50	3	0,50	3	0,50	0,10979	Very Low	0,10979	Very Low	0,21957	Low	0,21957	Low	0,21957	Low	0,21957	Low
0,36	Low	0,20	Low	4	0,75	5	1,00	5	1,00	5	1,00	5	1,00	5	1,00	5	1,00	0,5941	High	0,5941	High	0,5941	High	0,5941	High	0,5941	High	0,5941	High
0,22	Very Low	0,25	Low	4	0,75	5	1,00	5	1,00	5	1,00	5	1,00	5	1,00	5	1,00	0,28852	Moderate	0,28852	Moderate	0,28852	Moderate	0,28852	Moderate	0,28852	Moderate	0,28852	Moderate
0,35	Low	0,80	Very High	4	0,75	5	1,00	5	1,00	5	1,00	5	1,00	5	1,00	5	1,00	0,14478	Low	0,14478	Low	0,14478	Low	0,14478	Low	0,14478	Low	0,14478	Low
0,37	Low	0,70	High	2	0,25	3	0,50	3	0,50	4	0,75	4	0,75	4	0,75	4	0,75	0,08625	Very Low	0,08625	Very Low	0,12937	Low	0,12937	Low	0,12937	Low	0,12937	Low
0,37	Low	0,90	Very High	4	0,75	5	1,00	5	1,00	5	1,00	5	1,00	5	1,00	5	1,00	0,13425	Low	0,13425	Low	0,13425	Low	0,13425	Low	0,13425	Low	0,13425	Low
0,32	Low	0,55	High	5	1,00	5	1,00	5	1,00	5	1,00	5	1,00	5	1,00	5	1,00	0,19006	Low	0,19006	Low	0,19006	Low	0,19006	Low	0,19006	Low	0,19006	Low
0,35	Low	0,40	Moderate																										
0,60	Very High	0,60	High	1	0,00	1	0,00	1	0,00	1	0,00	1	0,00	1	0,00	2	0,25	0	Very Low	0	Very Low	0	Very Low	0	Very Low	0	Very Low	0,08269	Very Low
0,54	High	0,75	Very High	3	0,50	4	0,75	4	0,75	5	1,00	5	1,00	5	1,00	5	1,00	0,17794	Low	0,17794	Low	0,23726	Low	0,23726	Low	0,23726	Low	0,23726	Low

Map 1: Landslide Susceptibility Map of Taunggyi, Shan State, Myanmar. Baseline (Observed) Period

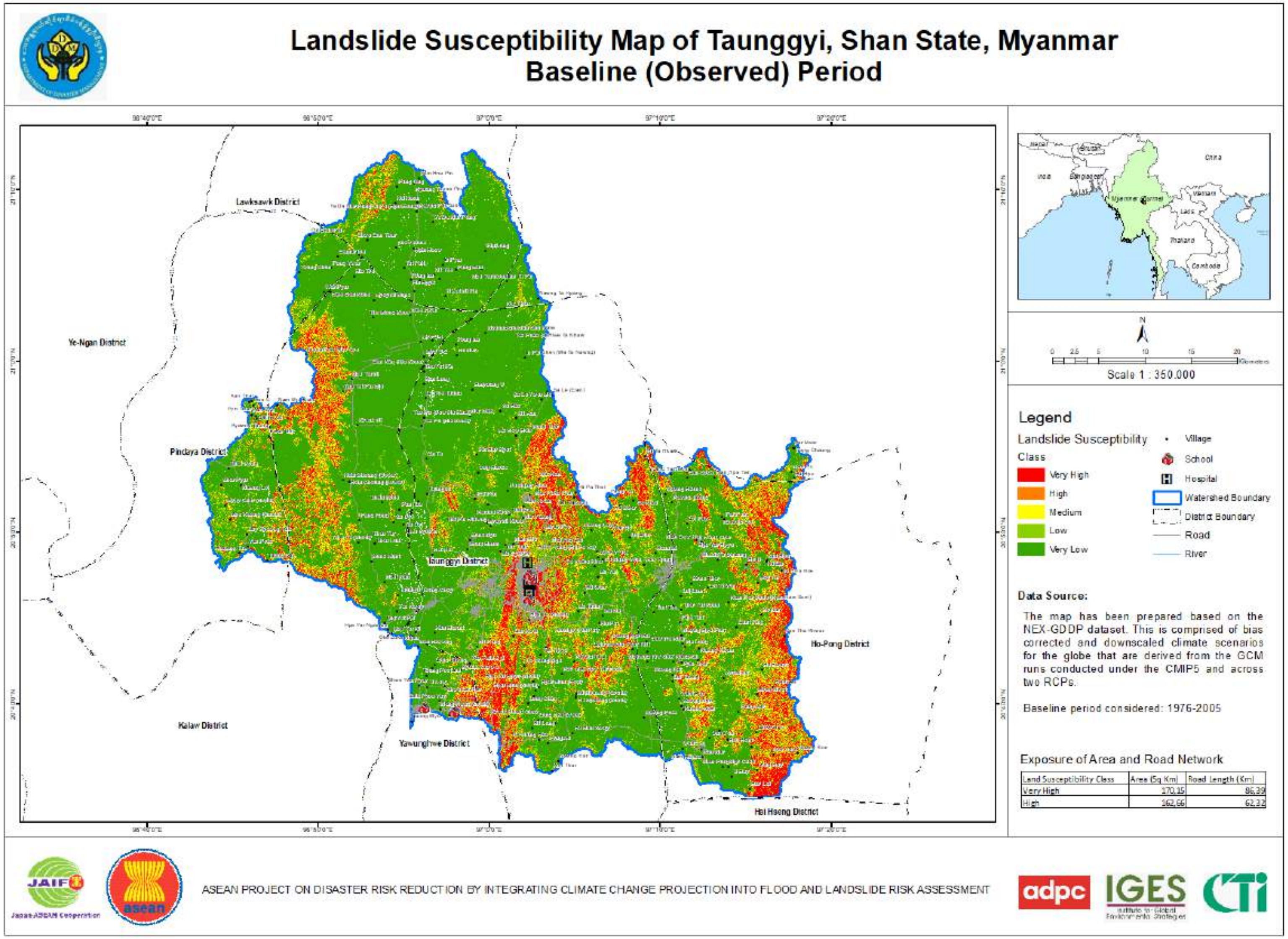

Map 2: Landslide Susceptibility Map of Taunggyi, Shan State, Myanmar. By 2030s based on the Highest Extreme GCM with RCP 4.5 Scenario

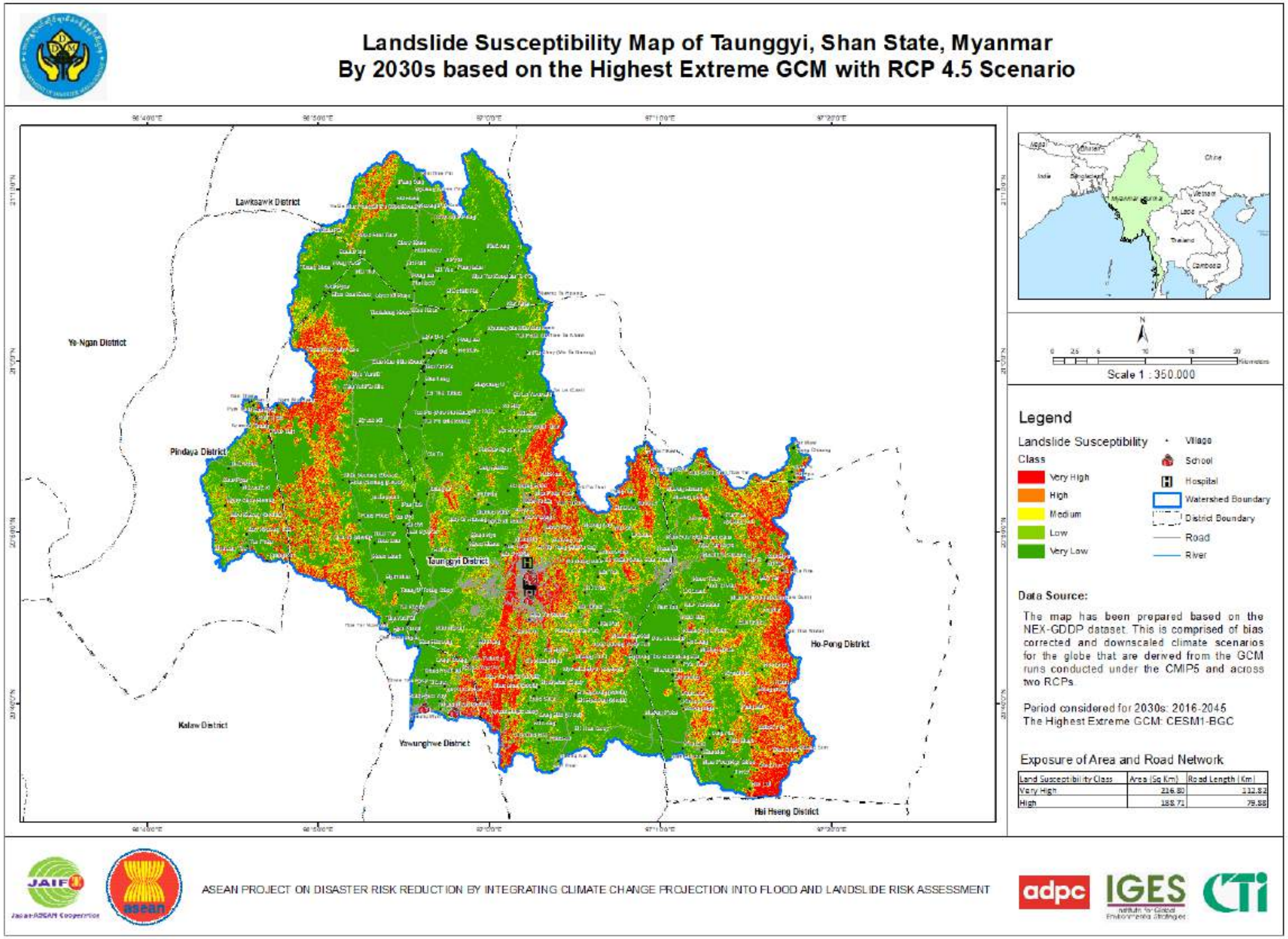

Map 3: Landslide Susceptibility Map of Taunggyi, Shan State, Myanmar. By 2030s based on the Highest Extreme GCM with RCP 8.5 Scenario

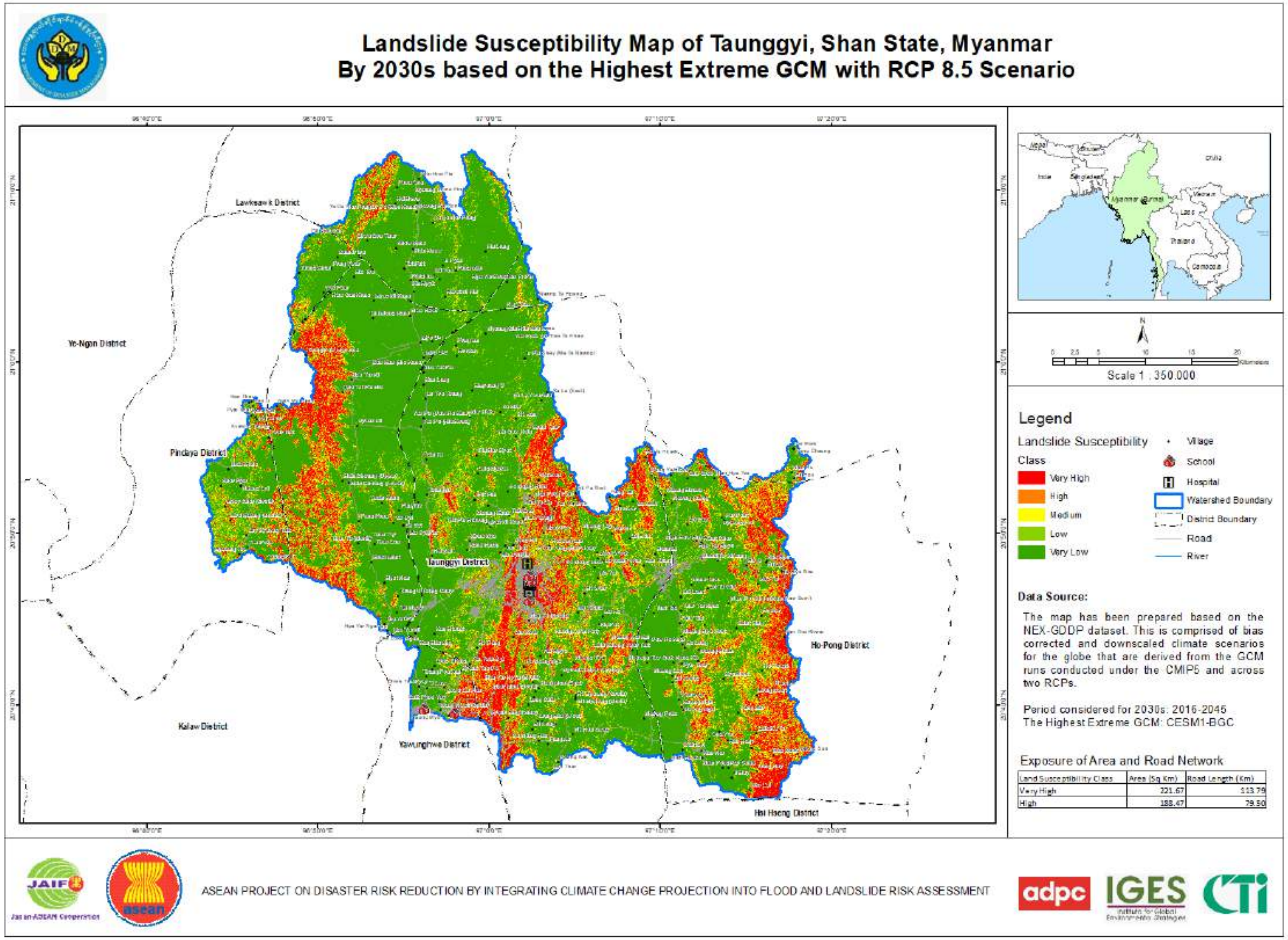

Map 4: Landslide Susceptibility Map of Taunggyi, Shan State, Myanmar. By 2050s based on the Highest Extreme GCM with RCP 4.5 Scenario

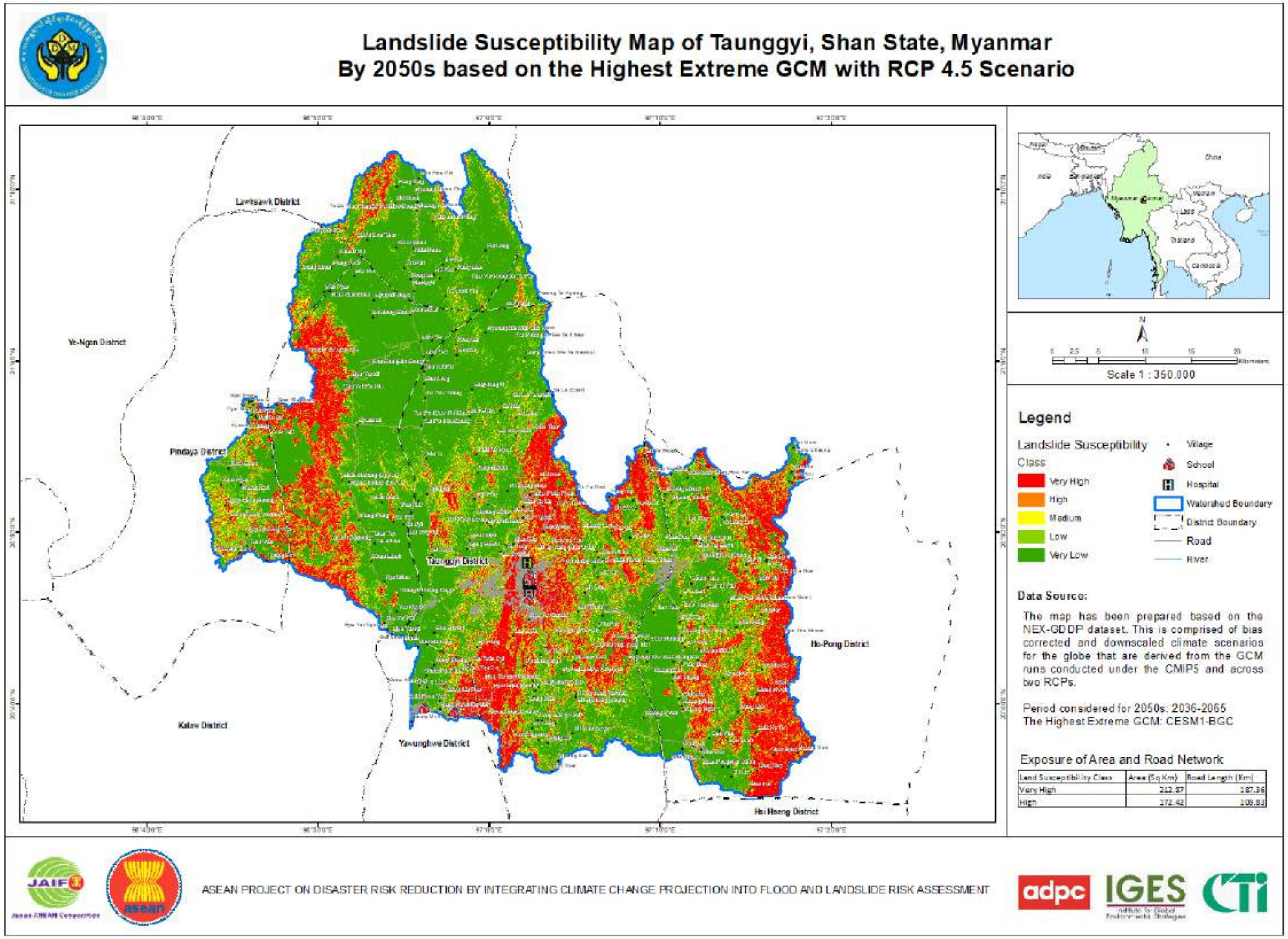

Map 5: Landslide Susceptibility Map of Taunggyi, Shan State, Myanmar. By 2050s based on the Highest Extreme GCM with RCP 8.5 Scenario

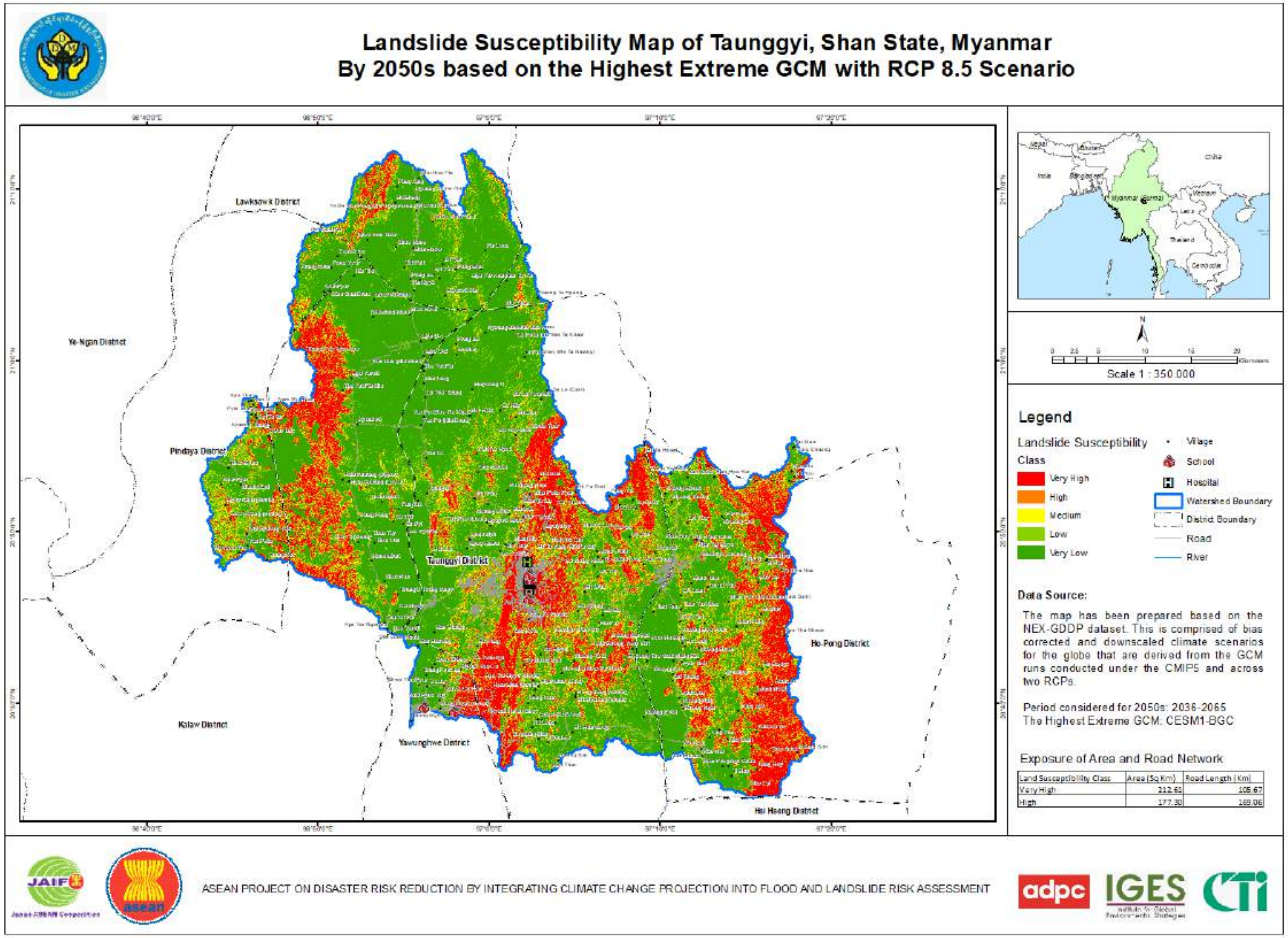

Map 6: Landslide Susceptibility Map of Taunggyi, Shan State, Myanmar. By 2080s based on the Highest Extreme GCM with RCP 4.5 Scenario

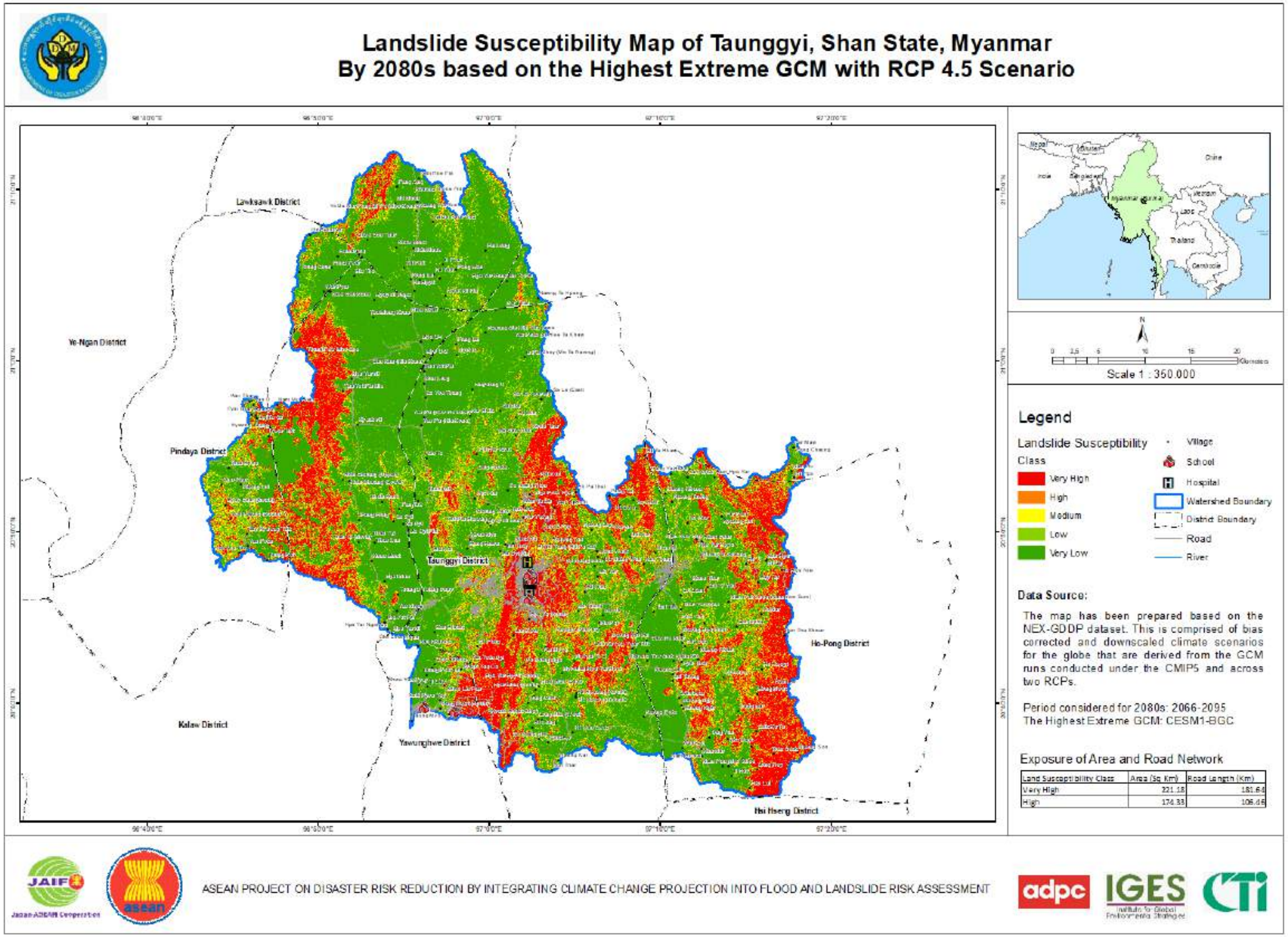

Map 7: Landslide Susceptibility Map of Taunggyi, Shan State, Myanmar. By 2080s based on the Highest Extreme GCM with RCP 8.5 Scenario

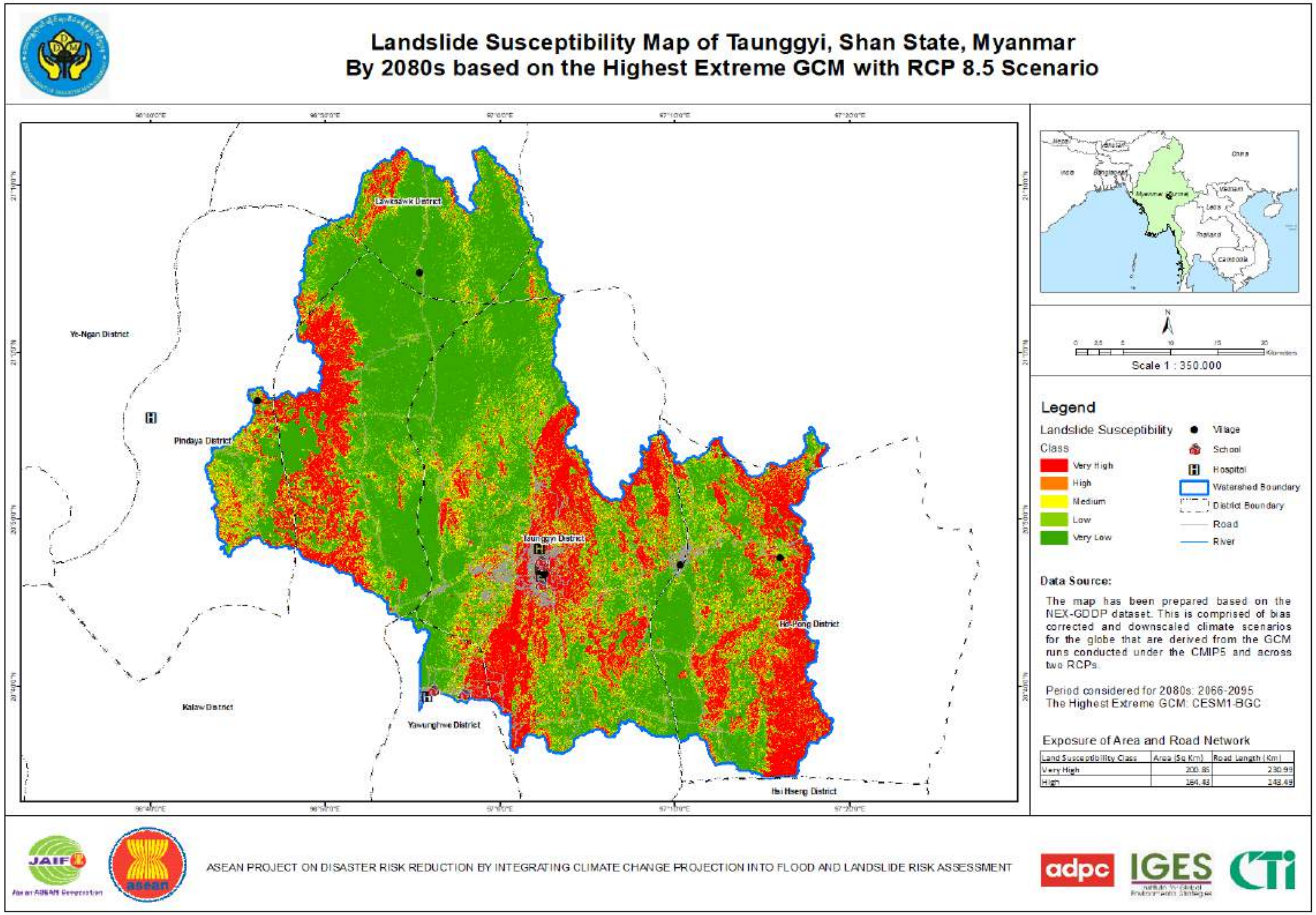

Map 8: Risk Distribution of Household Surveyed in Taunggyi Watershed of Shan State, Myanmar in 2019. Baseline (Observed) Period

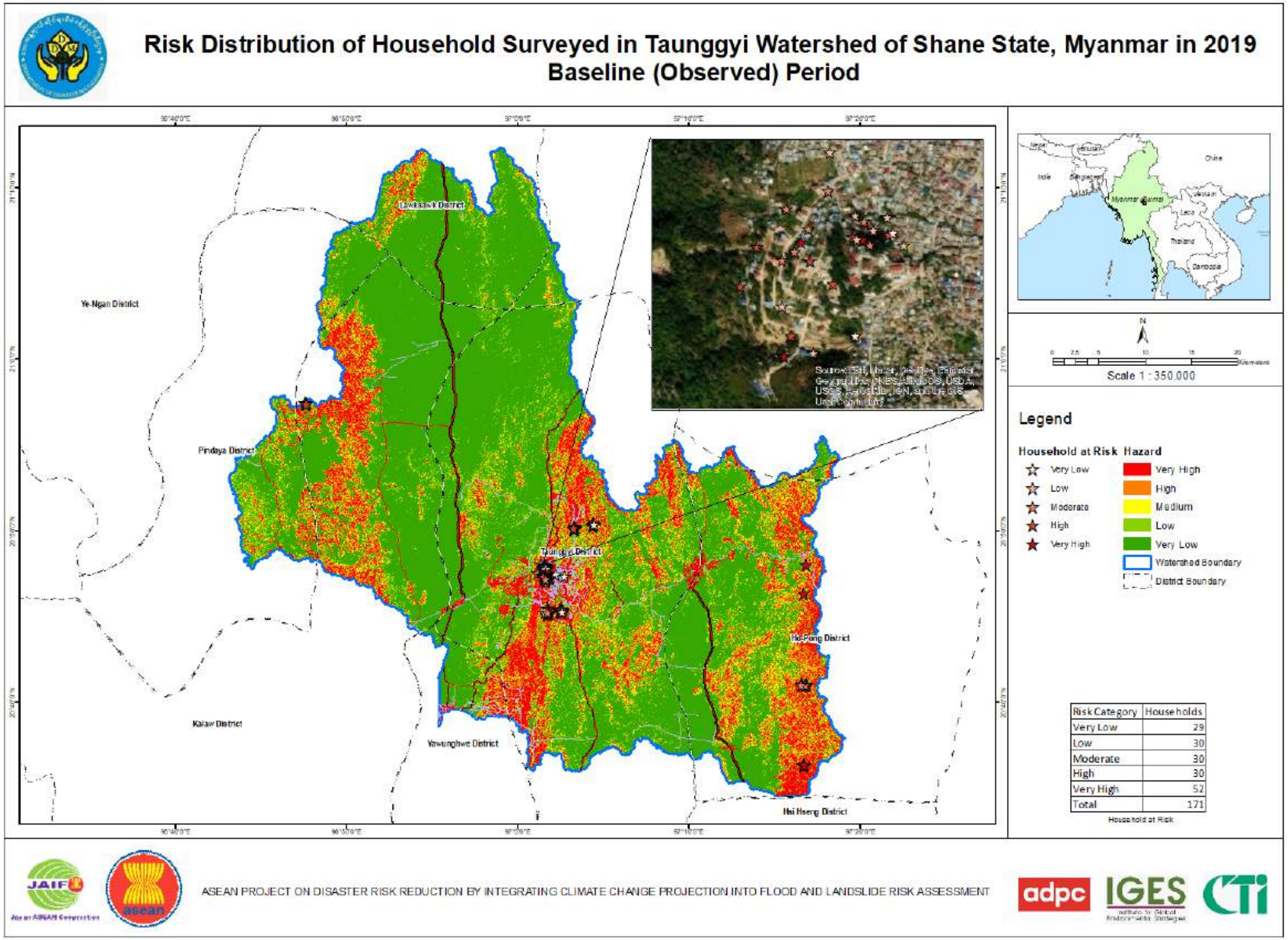

Map 9: Risk Distribution of Household Surveyed in Taunggyi Watershed of Shan State, Myanmar in 2019. By 2030s based on the Highest Extreme GCM with RCP 4.5 Scenario

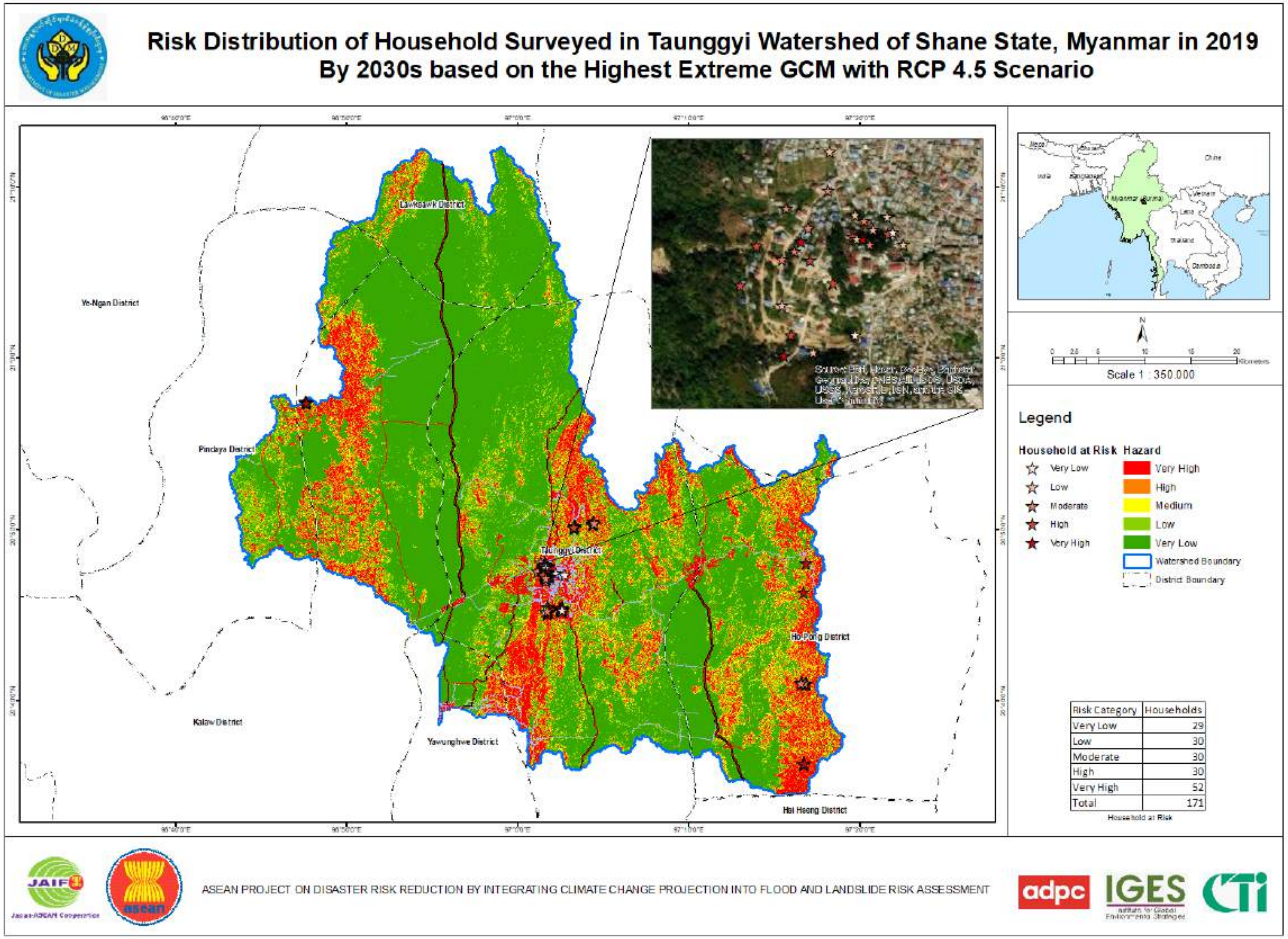

Map 10: Risk Distribution of Household Surveyed in Taunggyi Watershed of Shan State, Myanmar in 2019. By 2030s based on the Highest Extreme GCM with RCP 8.5 Scenario

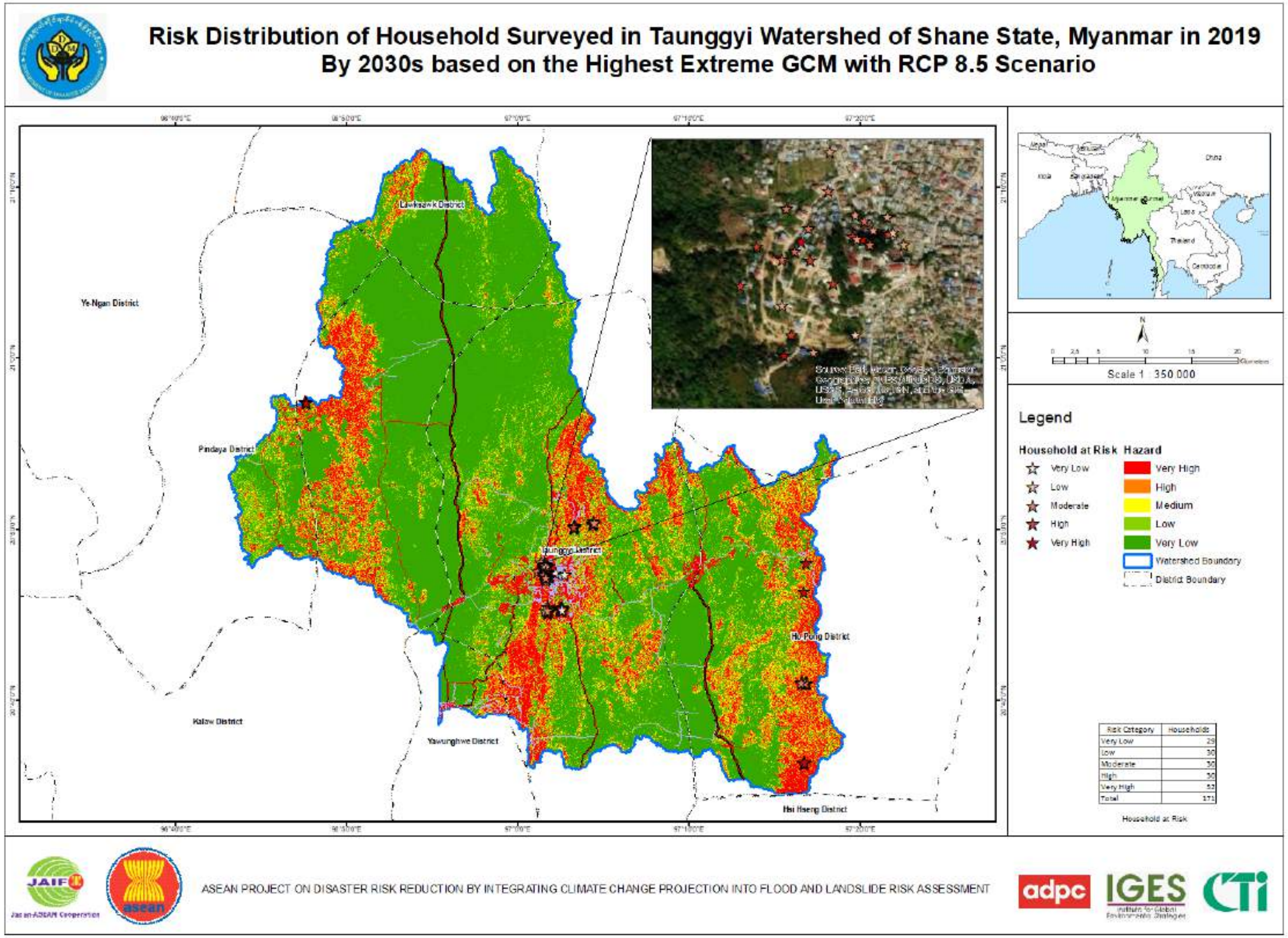

Map 11: Risk Distribution of Household Surveyed in Taunggyi Watershed of Shan State, Myanmar in 2019. By 2050s based on the Highest Extreme GCM with RCP 4.5 Scenario

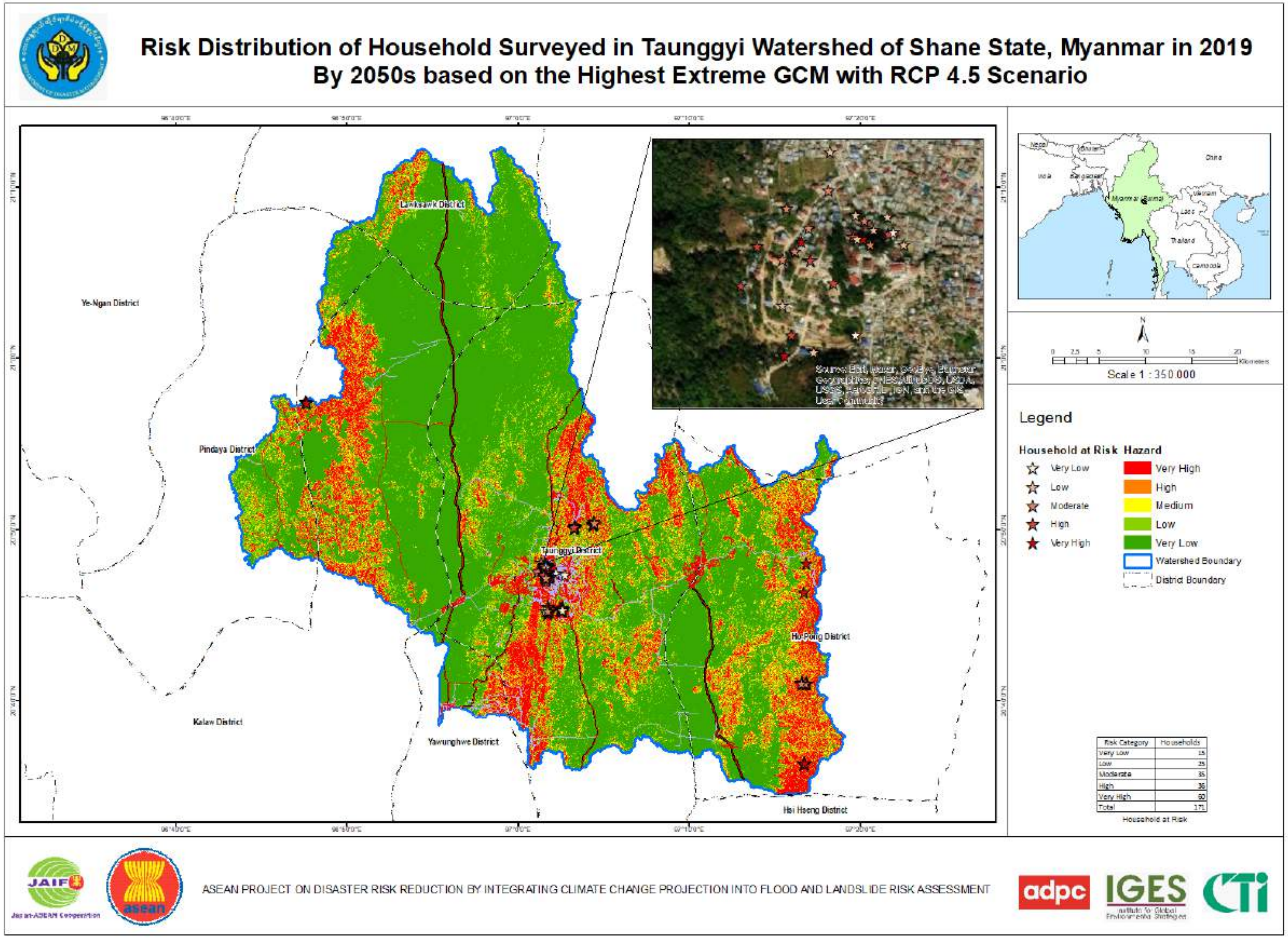

Map 12: Risk Distribution of Household Surveyed in Taunggyi Watershed of Shan State, Myanmar in 2019. By 2050s based on the Highest Extreme GCM with RCP 8.5 Scenario

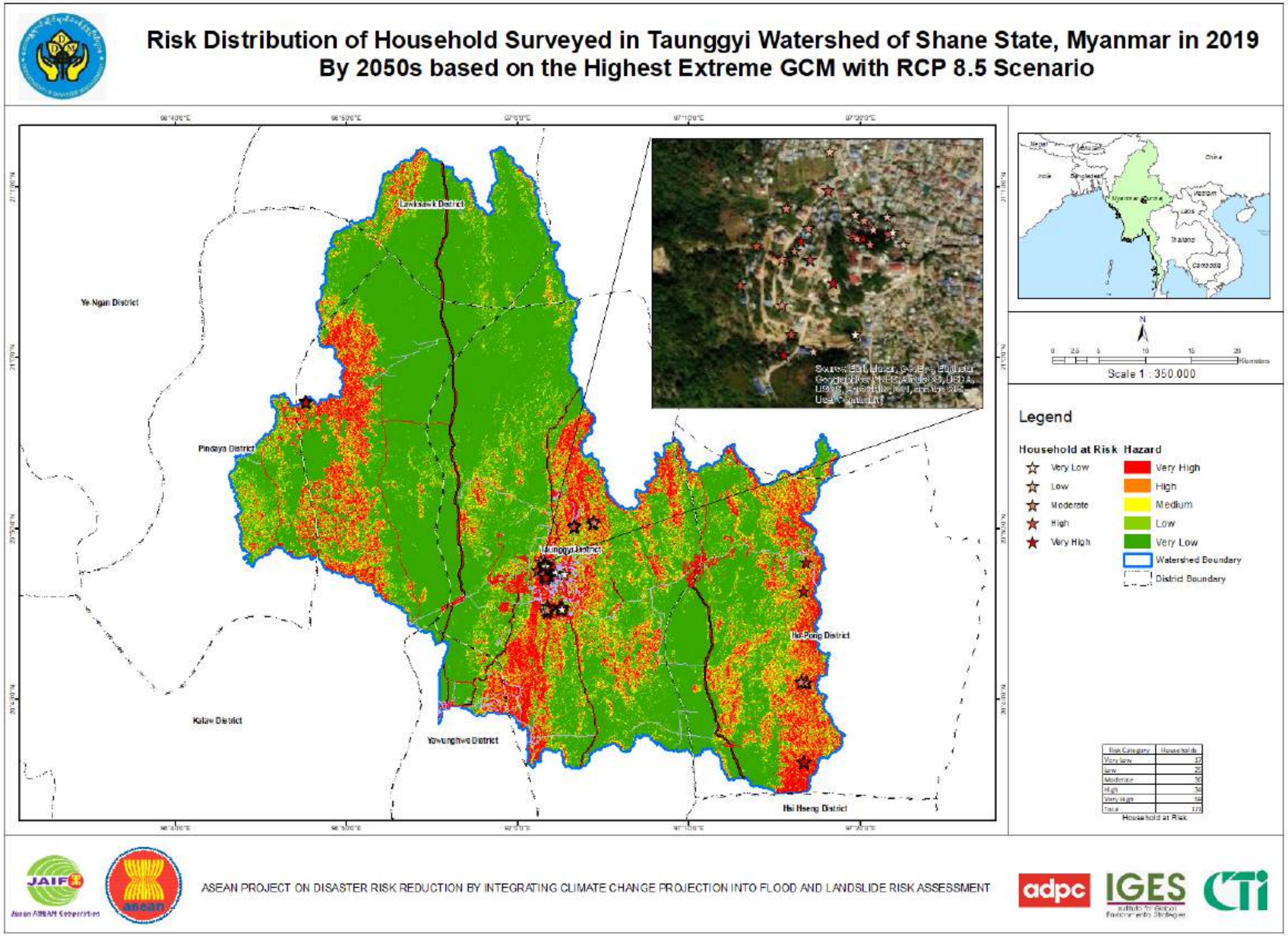

Map 13: Risk Distribution of Household Surveyed in Taunggyi Watershed of Shan State, Myanmar in 2019. By 2080s based on the Highest Extreme GCM with RCP 4.5 Scenario

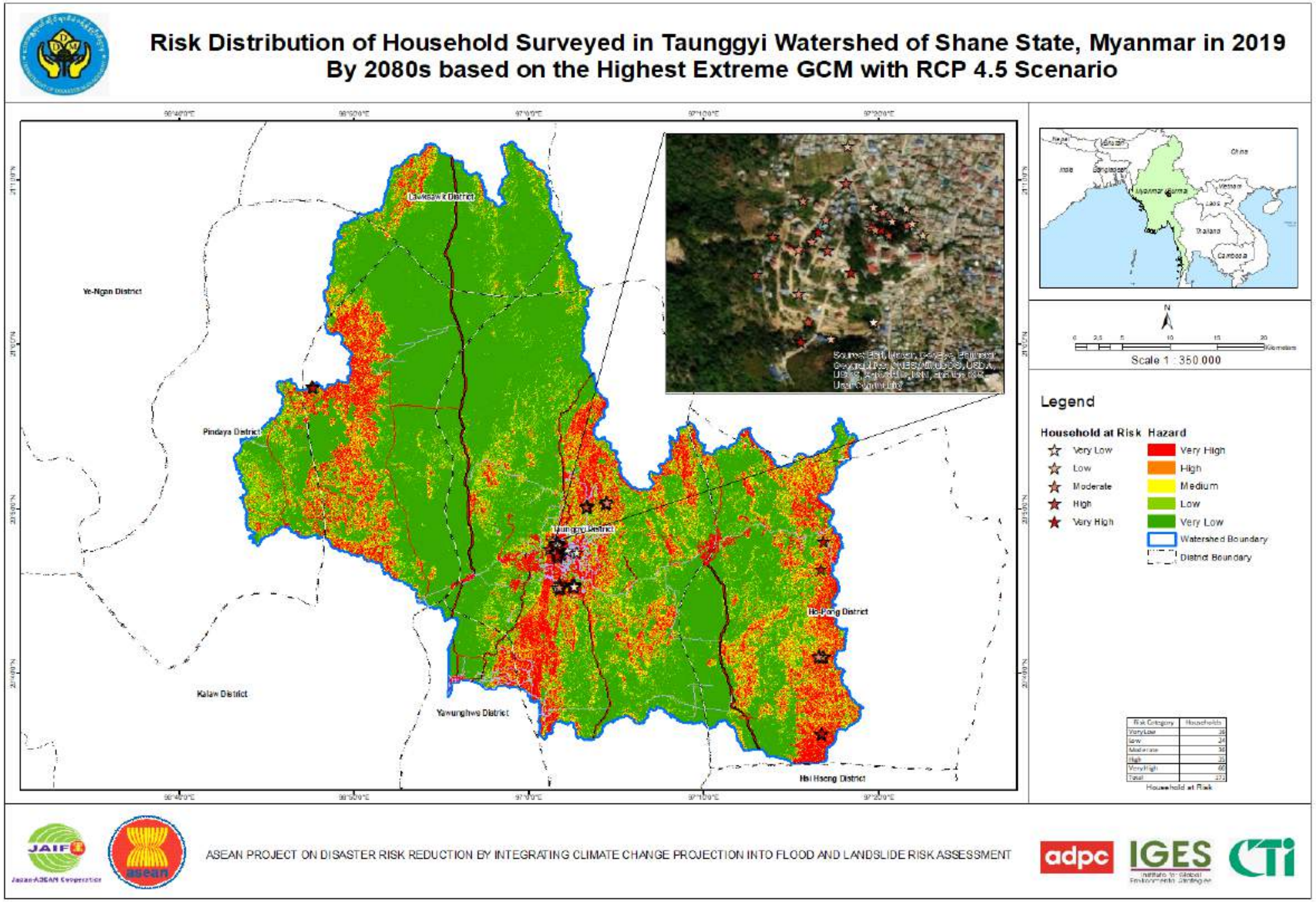

Map 14: Risk Distribution of Household Surveyed in Taunggyi Watershed of Shan State, Myanmar in 2019. By 2080s based on the Highest Extreme GCM with RCP 8.5 Scenario

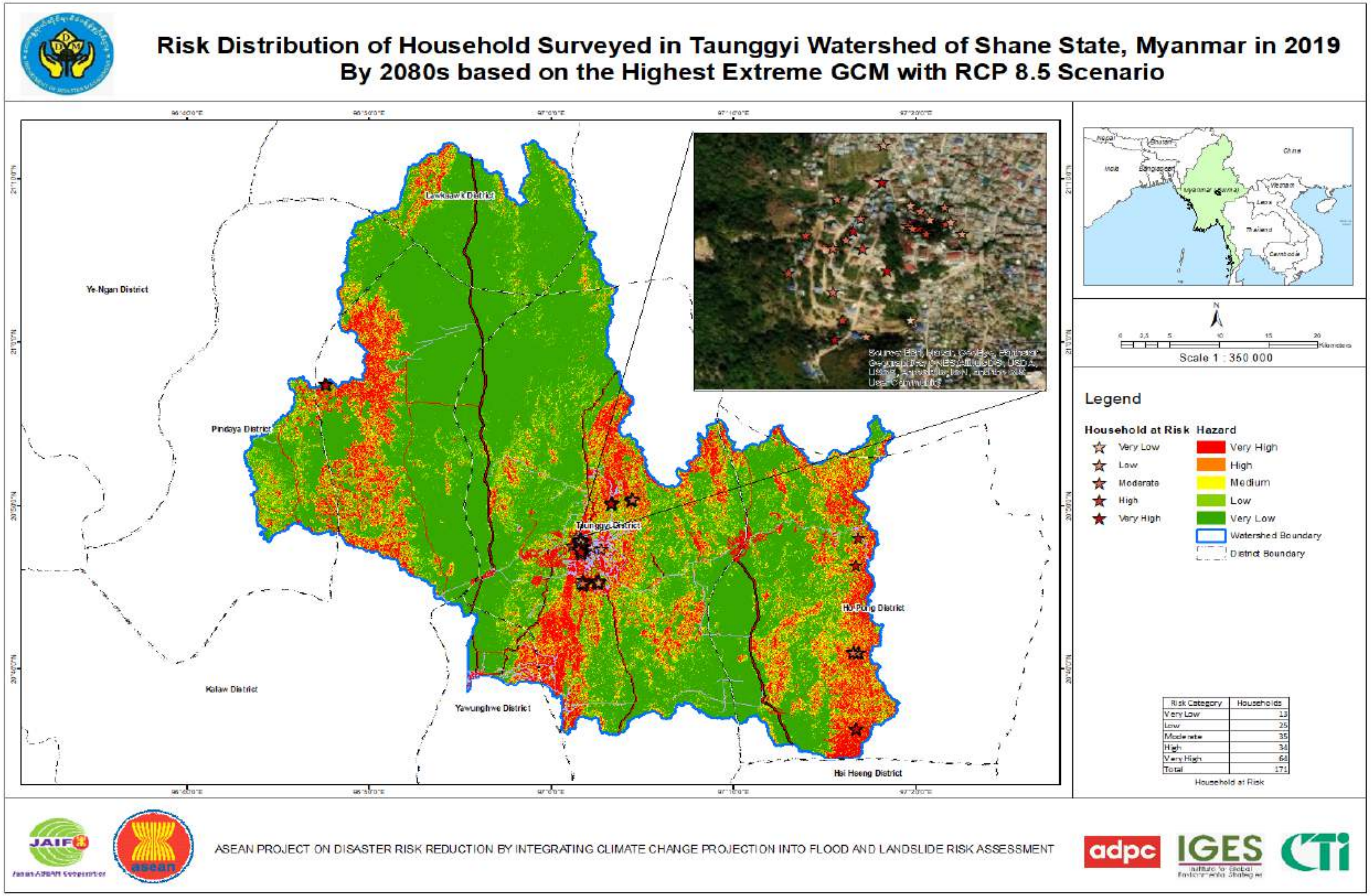

Map 15: Capacity Distribution of Household Surveyed in Taunggyi, Shan State, Myanmar (2019)

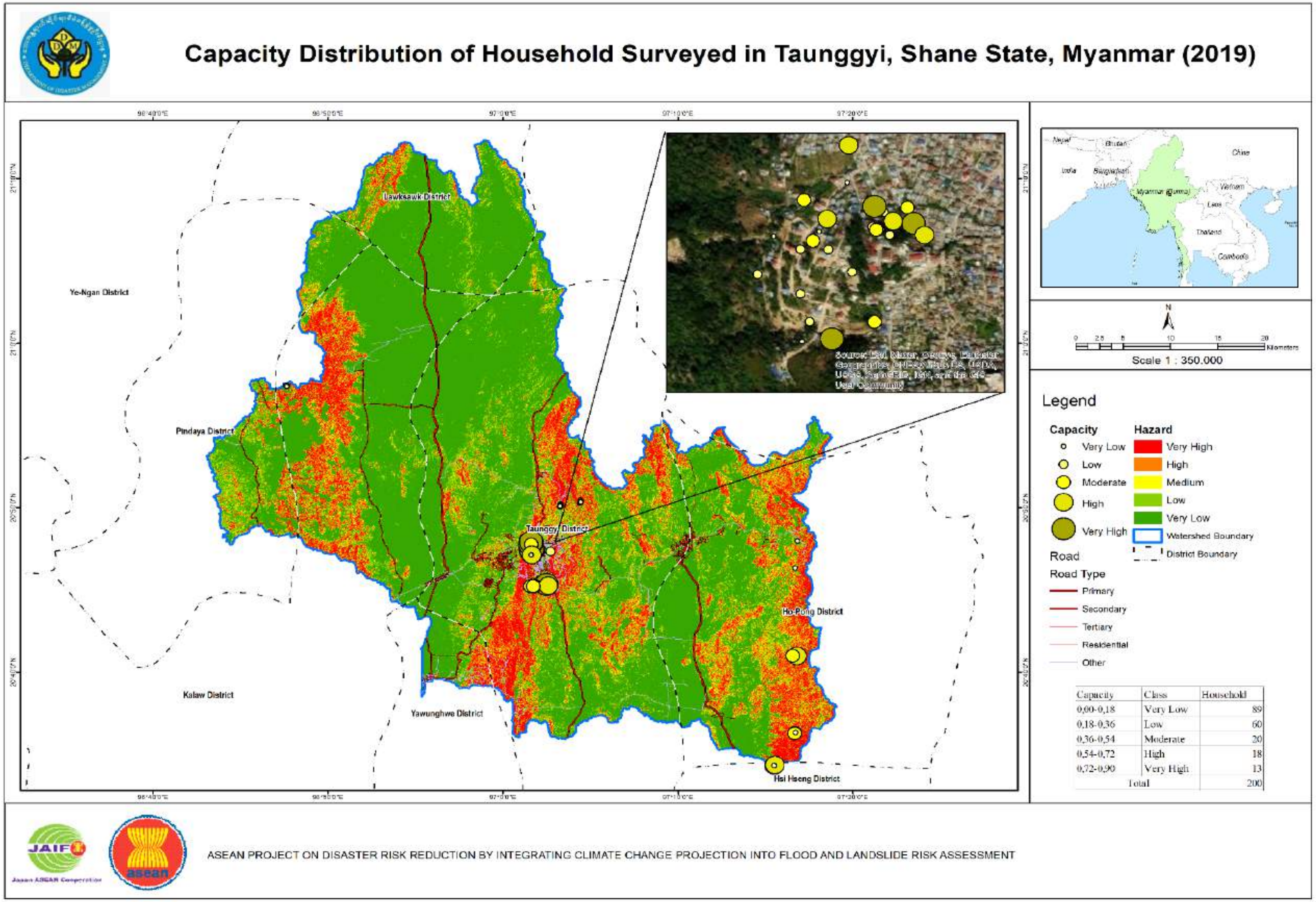

Capacity	Class	Household
0,00-0,18	Very Low	89
0,18-0,36	Low	60
0,36-0,54	Moderate	20
0,54-0,72	High	18
0,72-0,90	Very High	13
Total		200

Map 16: Vulnerability Distribution of Household Surveyed in Taunggyi, Shan State, Myanmar (2019)